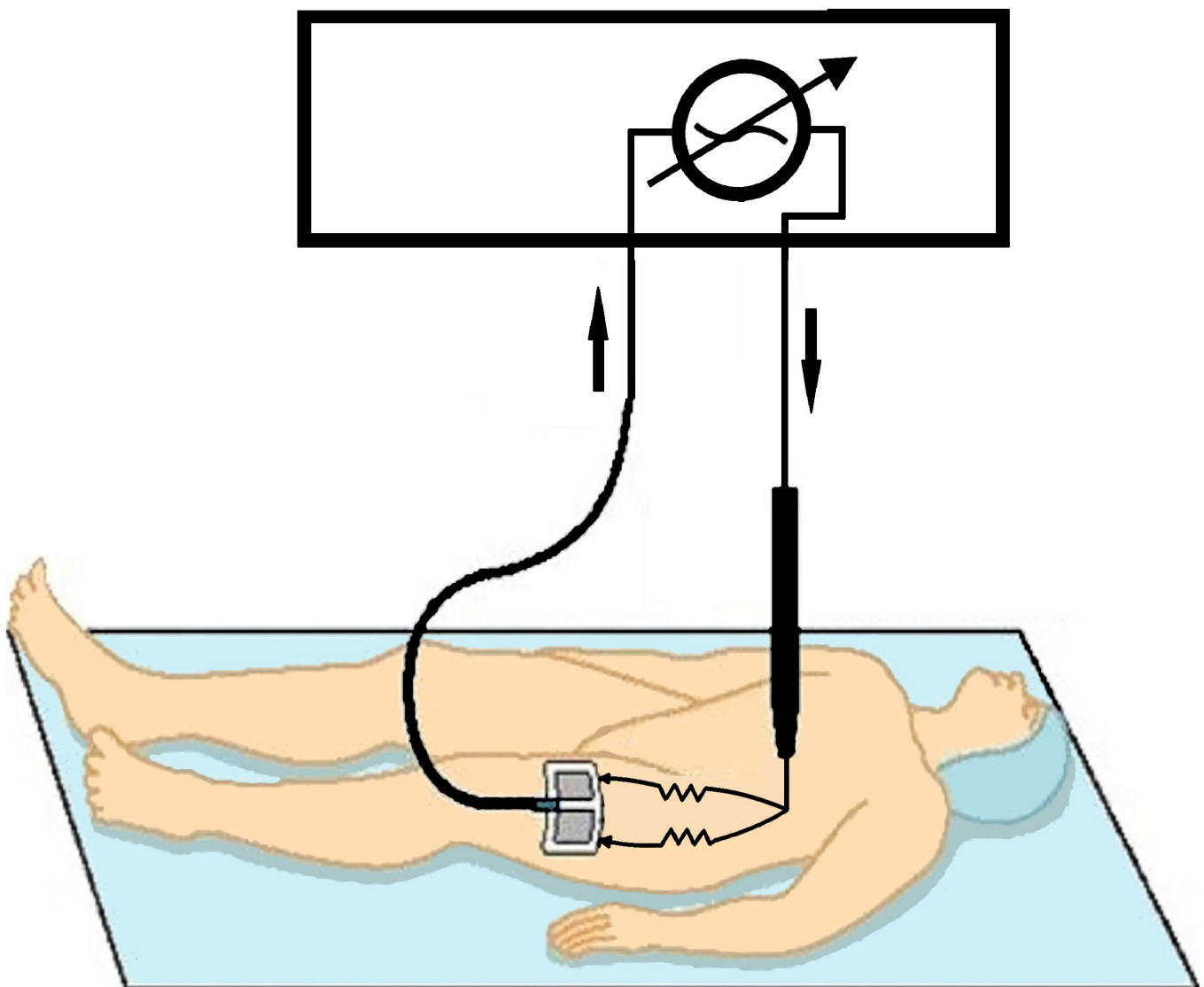# Critical Design Requirements for an Electrosurgical Unit used in Low-Middle Income Countries

by

Felix Cranz

Critical Design Requirements for an Electrosurgical Unit used in Low-Middle Income Countries

by

Felix Cranz

to obtain the degree of Master of Science
at the Delft University of Technology,
to be defended publicly on Tuesday March 12, 2018 at 14:00 AM.

Student number: 4718470
Project duration: August 20, 2017 – March 12, 2018
Thesis committee: Prof. Dr. ir. J. Dankelman,   TU Delft, supervisor
                    Dr. ir. L. S. G. L. Wauben,   TU Delft
                    Dr. ir. J. C. Diehl,   TU Delft

This thesis is confidential and cannot be made public until March 12, 2023.

"If you don't have an competitive edge, don't compete"

-Jack Welsh

Summary

Introduction: Over five billion people in mainly low and middle income countries (LMICs) do not have access to safe surgery. This is due to a lack of available and functional medical equipment, where up to 70% of the existing equipment is broken. Some reasons for this shortage in medical equipment are a lack of funding, maintenance, training, educated procurement and infrastructure. To improve access to affordable quality equipment in LMICs, the design of a low cost and high quality Electrosurgical unit (ESU) is suggested. An ESU is an essential operating tool to assist surgeons on various operations. To start the design process, critical design requirements are laid out in this paper based on the properties and thermal performance of three existing devices.

Theoretical Background: Electrosurgery is used in various operations to cut and coagulate tissue through high frequency current. By changing the power intensity and waveform of the current, tissue can be heated to different levels. The coagulation of tissue occurs between 60–100°C, while vaporization occurs >100°C. Hazards in electrosurgery include current leakage and the detachment of the return electrode, which can cause burns to the user, staff or patient.

Methods: The design requirements were obtained by conducting experiments and comparing three ESUs. Two of the ESUs are regarded as high-end devices, while the third, due to a low price and a simplified design, can be seen as a low-end device. Through a Property Test and a Thermal Camera Test, cut and coagulation modes were tested for each electrosurgical device at different powers and loads. For the Property Test the power, waveforms, crest factor, current and voltage at activation were measured and analysed. To understand the effects of the measured properties, a thermal camera was used to measure the heat map on tofu samples (simulating human tissue) that were exposed to currents from each of the three ESUs.

Results: The actual power was measured to be lower than the set power at rated loads for all three ESUs. The wave-shape of all three devices differed considerably, producing a different thermal output on the tofu samples. All devices dropped their power with an increase in load. One ESU exceeded the $100\,\mathrm{mA}$ current leakage limit set by standards. In the Thermal Camera Test, high end devices produced temperature values more similar to those expected from literature.

Discussion: The most important design requirements to consider include an efficient waveform design and a steady power control. With a small, light weight, and repairable hardware using sterilisable accessories, the ESU would become more transportable, robust, and independent from the manufacturer; therefore also more suitable for a LMICs. A split return electrode and low leakage are important design criteria to prevent any injury to patients and users. Improvements to the study include a wider pool of different ESUs for a better market analysis, using a camera with a higher temperature measurement than 177°C and larger tofu samples for a better thermal analyses.

ACKNOWLEDGMENT

CONTENTS

LIST OF ABBREVIATIONS

AC	Alternating Current
CF	Crest Factor
Coag	Coagulation
DC	Duty Cycle
ERBE	ERBE ICC 300
ESU	Electrosurgical Unit
HICs	High income countries
HF	High Frequency
IRT	Instant Response Technology
LMICs	Low and Middle Income Countries
RDE	RDE Electrocut 100
RMS	Root mean square
Valleylab	Valleylab Force FXc
Vall	Valleylab Force FXc

NOMENCLATURE

A	Area
a	Side length of a pixel
f	Frequency
I	Current
J	Current Density
L	Load
l	Length
P	Power
P_{max}	Maximum Power
pw	Pulse Width
$Pxls$	Number of selected pixels
S	Test Sequence
σ	Electrical conductivity
T	Temperature
T_{max}	Absolute maximum temperature measured over activation
$mean\ T_{max}$	The mean of all maximum temperatures at each time point over the activation period
t	Time
V_{pp}	Voltage peak-to-peak
x_p	Peak value
x_{RMS}	Root mean square value

Critical Design Requirements for an Electrosurgical Unit used in Low-Middle Income Countries

Felix Cranz

Abstract—**Introduction: Over five billion people in mainly low and middle income countries (LMICs) do not have access to safe surgery. This is due to a lack of available and functional medical equipment, where up to 70% of the existing equipment is broken. Some reasons for this shortage in medical equipment are a lack of funding, maintenance, training, educated procurement and infrastructure. To improve access to affordable quality equipment in LMICs, the design of a low cost and high quality Electrosurgical unit (ESU) is suggested. An ESU is an essential operating tool to assist surgeons on various operations. To start the design process, critical design requirements are laid out in this paper based on the properties and thermal performance of three existing devices.**
Theoretical Background: Electrosurgery is used in various operations to cut and coagulate tissue through high frequency current. By changing the power intensity and waveform of the current, tissue can be heated to different levels. The coagulation of tissue occurs between 60–100°C, while vaporization occurs >100°C. Hazards in electrosurgery include current leakage and the detachment of the return electrode, which can cause burns to the user, staff or patient.
Methods: The design requirements were obtained by conducting experiments and comparing three ESUs. Two of the ESUs are regarded as high-end devices, while the third, due to a low price and a simplified design, can be seen as a low-end device. Through a Property Test and a Thermal Camera Test, cut and coagulation modes were tested for each electrosurgical device at different powers and loads. For the Property Test the power, waveforms, crest factor, current and voltage at activation were measured and analysed. To understand the effects of the measured properties, a thermal camera was used to measure the heat map on tofu samples (simulating human tissue) that were exposed to currents from each of the three ESUs.
Results: The actual power was measured to be lower than the set power at rated loads for all three ESUs. The wave-shape of all three devices differed considerably, producing a different thermal output on the tofu samples. All devices dropped their power with an increase in load. One ESU exceeded the $100\,\mathrm{mA}$ current leakage limit set by standards. In the Thermal Camera Test, high end devices produced temperature values more similar to those expected from literature.
Discussion: The most important design requirements to consider include an efficient waveform design and a steady power control. With a small, light weight, and repairable hardware using sterilisable accessories, the ESU would become more transportable, robust, and independent from the manufacturer; therefore also more suitable for a LMICs. A split return electrode and low leakage are important design criteria to prevent any injury to patients and users. Improvements to the study include a wider pool of different ESUs for a better market analysis, using a camera with a higher temperature measurement than 177°C and larger tofu samples for a better thermal analyses.

Keywords—*Electrosurgery, Erbe, Valleylab, RDE, LMICs.*

I. INTRODUCTION

Safe surgery is not accessible to over five billion people in mainly low and middle income countries (LMICs) [1] [1] due to a lack of medical access, cost and specialists [2]. A lack of existing or functioning medical equipment is a major factor preventing reliable diagnostics and surgical interventions [3].

With capital cost being a main barrier to purchasing equipment, donations of used equipment is common [4]. However, often training for the donated equipment is missing, spare parts are not made anymore or prohibitively expensive. Even if spare parts were affordable, the hospitals may not have the expertise to execute the repair [3]. Furthermore, manuals are often lost in the donation process or the manuals are not of the indigenous language. Hence, maintenance is an essential problem in LMICs, where today around 70%–80% of equipment is non-functional within 5 years after acquiring [5].

Bad procurement is also at the heart of the issue [4]. A lack of regulatory authorities, biomedical engineers, and due to corrupt politicians, equipment is bought that is not necessarily robust enough to be deployed in harsh conditions. Often devices are not transportable to remote regions, cannot function at high ambient temperatures, and cannot tolerate grid fluctuations [4] [3].

The spread of disposable equipment, where reusable alternatives exist, is a difficult barrier to overcome [3]. Besides the problem of availability of the disposables in a LMIC setting, disposables are also more expensive in the long run. When compared to high-income countries, the labour cost in LMICs is much lower, allowing for the cleaning of reusable to effectively be cheaper [3].

As a step towards improving surgical care and access to affordable medical equipment in LMICs communities, high quality low cost Electrosurgical Units (ESUs) are needed.

ESUs are used as an essential operating tool to assist the surgeon for many surgical procedures [6]. By heating target tissue through high frequency (HF) electrical current, different types of tissues can be cut and coagulated using a metallic instrument or needle [7]. The user selects the power intensity on the device. Once activated, the current then runs from the active to the neutral electrode through the body, where the body is represented as a resistive load in Figure 1. The advantage of electrosurgery in a LMICs setting is that it is widely applicable, helps to stop and prevent bleeding, allows for precise cutting, and facilitates better wound healing in
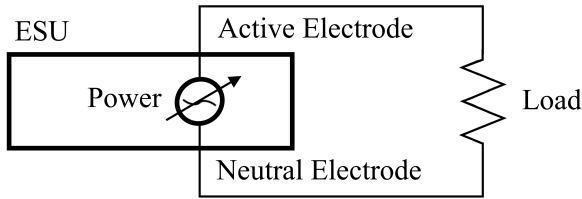
---

less hygienic environments [8].

Fig. 1: A basic sketch of an ESU. Power can be set on the device and the patient acts as a resistive load between the active and neutral electrodes.

The market today is dominated by high-end ESUs characterized by high prizes, large number of settings and computer control systems. A few low-end devices also exist that—due to their stripped down, fully analogue and simple design—are cheaper, more transportable and robust.

To design a new ESU that fits into a LMICs setting, critical design requirements are necessary. These requirements determine what is needed to allow for the future design or—if more feasible—the purchase of an ESU that is

- robust,
- transportable,
- effective,
- affordable
- safe,
- repairable,
- equipped with reusable accessories,
- have a simple usability, and
- a low maintenance.

Four areas of investigation have been identified to determine design requirements for an ESU in a LMICs setting. (1) a technical analyses of the properties, which includes investigating the physical properties of current devices such as robustness, transportability, effectiveness, cost and functional reliability; (2) safety for user, staff and patient; (3) repairability and maintenance; and (4) usability for the surgeon. Through a selection process (Appendix A, pg. 23) it was decided to lay the focus of this study only on the first two areas of investigation—namely the technical and safety aspects of the ESUs. Therefore repairability, maintenance and usability are out of the scope of this study.

For a better understanding of current devices and their technical and safety standards, an evaluation of one low-end and two high-end ESUs was made to find out how their features for monopolar open surgery compare: (1) *Valleylab Force FXc* (Medtronic, USA), (2) *ERBE ICC 300* (ERBE Medizintechnik GmbH, Germany), (3) *RDE Electrocut 100* (Recherche Développement Electronique, France).

For a technical and safety analysis of the ESUs, reverse engineering was made by exploring their respective design properties. To understand these design properties the thermal effectiveness of the ESUs was tested and explored on tofu samples. The results were used to find critical design requirements for an improved or new ESU design aimed for a LMICs setting.

II. THEORETICAL BACKGROUND

Electrosurgery is the use of high frequency (HF) alternating current (AC) at frequencies typically between 300 kHz–1 MHz to raise intracellular temperature [9]. This effect is mainly used for the cutting and coagulation (stop bleeding) of tissue [10]. These functionalities are used in general open surgery as well as minimally invasive surgery, allowing for a wide range of applications [11]. The use of electrosurgery ranges from abdominal surgeries to dermatology [12], from stomatology [13] [6] to ophtamology [6], from oto-rhino-laryngology [14] [15] to orthopaedic surgeries [13] and many more surgical fields.

(a) Monopolar Electrosurgery

(b) Bipolar Electrosurgery
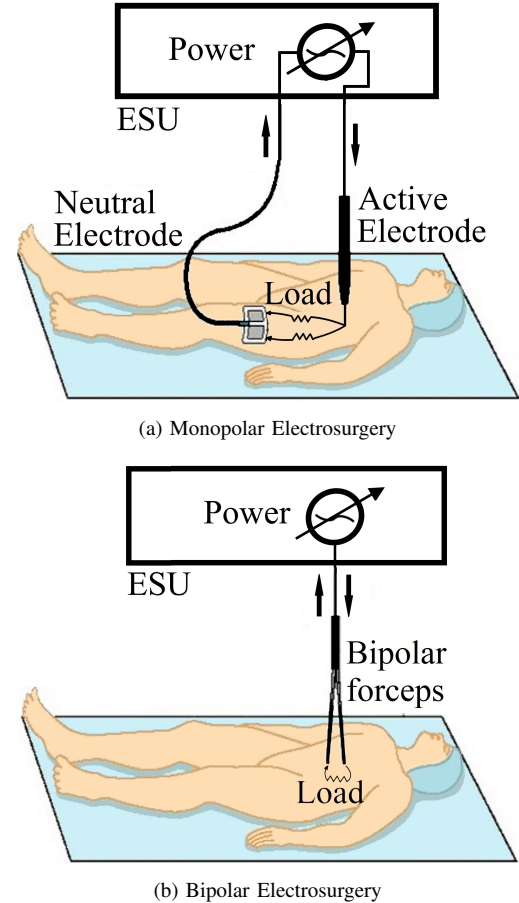
Fig. 2: (a) In monopolar surgery the current flows from the active electrode to the neutral electrode pad. (b) For Bipolar surgery the current flows between two electrodes on the same operation tool, such as tweezers. In both cases the human body acts as a resistive load.

Electrosurgery can be performed using either a monopolar or a bipolar instrument [7] [9]. For monopolar electrosurgery, a pad with a large surface area, the neutral dispersive electrode, is placed on a strategic part of the body (See Figure 2a). The circuit is closed at the point of surgical interest through an electrode tool with a much smaller surface area called the active electrode [9], [15]–[17]. For bipolar electrosurgery

(Figure 2b), the target tissue is placed between the electrodes (e.g. tweezers). Current flows through the clasped tissue, closing the circuit and resulting in the target tissue to become coagulated or cut [15] [17].

Monopolar surgery is more commonly used than bipolar surgery [18]. Furthermore, minimally invasive surgery (for which primarily bipolar tools are used) is rare in LMICs because the neccesary infrastructure is often missing (such as endoscopes, screens, a hygienic environment and trained staff) [19].

As indicated in Figures 2, the human body acts as a resistive load in electrosurgery. Depending on the distance between the electrodes and the type of tisse, this load ranges from $100\,\Omega/\mathrm{cm}$ (Brain (gray matter)) to over $3000\,\Omega/\mathrm{cm}$ (Bone) [20]. Most ESUs have an optimal load they can operate at (rated load) of between $200-300\,\Omega$ depending on their application [21]. With an increasing load, however, an ESU usually experiences a power drop, resulting in a lower thermal performance. For the surgeon to be able to predict the thermal outcomes during a procedure, the ideal ESU does not change its power output regardless of the load.

The main settings the surgeon varies during a procedure are the power level and waveform (cut and coagulation), but current density, points of current entry and exit, the power level and frequency also influence the thermal effect and the clinical outcome of the electrosurgical device on tissue. [22].

Current density J is defined as the cross-sectional area A through which the current I flows ($J = I/A$). Current density J is proportional to the square of the tissue heat ($H = J^2 L$), with L representing the load of the tissue [16]. Thus, the smaller the active electrode through which the HF current flows, the stronger the thermoelectric effect.

The high frequency AC wave properties are the main cause for tissue heating [16]. Inside the cell, there are positively as well as negatively charged ions and particles. When the current has a positive polarity, the ions and particles are attracted to the opposite pole, gathering on one side of the cell. This process is reversed when the polarity of the current changes to negative, causing movement in the cell as the ions rush to the other side. At a high frequency this migration of ions occurs very fast, causing frictional heat and consequently raising the intracellular temperature [9]. To achieve a clear change in polarity, a clean sinusoidal waveform is needed to achieve a clear change in polarity and therefore a strong attraction force for ions and particles.

The typical cut and coagulation waveforms can be seen in Figure 3. For the cut mode a continuous, ideally sinusoidal, waveform at low peak-to-peak voltages (V_{pp}) heats tissue to high temperatures. The quality of the waveform is measured with the crest factor (CF), which is the ratio between a peak value and the effective RMS value ($CF = \frac{X_P}{X_{RMS}}$) [23] [9]. For a perfect sinusoid the $CF = \sqrt{2}$, while higher values indicate more extreme peaks. To achieve coagulation, the waveform design ideally has a high voltage duty cycle (DC), which is the pulse width pw over total time ($DC = \frac{pw}{t}$). With a duty cycle the tissue has the chance to cool between bursts of high current. These cooling periods can be modified in relation to the current bursts to control the tissue temperatures [10].
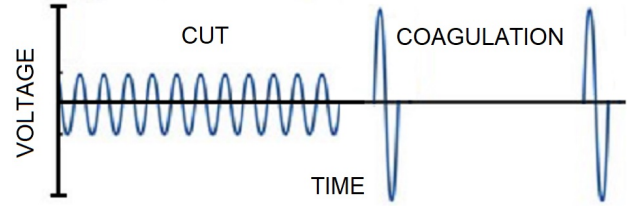

Fig. 3: The typical cut and coagulation waveforms. Cut: continuous & low V_{pp}. Coagulation: current bursts & high V_{pp}.

The tissue response with electrosurgical devices can largely be predicted with reliable and known mechanical and thermal interactions [24]. By being able to control the heating of the tissue to different levels of temperatures, various effects can be achieved in surgery.

At 50°C cells will die after being exposed for 6 minutes. At a temperature between 60–99°C, protein denaturation is initiated and the cell dies immediately, dessicating and shrinking [9]. When coagulating tissue this temperature range is aimed to be reached with a large area affected to stop bleeding or to seal vessels.

When the cell reaches over 100°C, the cytoplasm expands rapidly due to gas formation—vaporizing the cell [15]. As soon as a cell touches the active electrode it vaporizes, causing a clean scalpel-like cut, with a small area of thermal damage [9].

At above 200°C organic molecules break down in a process called carbonization, leaving a black or brown layer of carbon molecules. [17]. Carbonization makes the electrode adhere to the tissue, causing the eschar to be pulled off when removing the electrode, resulting in bleeding. Hence these temperatures are avoided when the electrode is in direct contact with the tissue [9].

Due to the high energy used for electrosurgery, it has dangers and hazards that need to be accounted for. Two important safety aspects are HF current leakage and dispersive electrode detachment in monopolar surgery.

When current takes alternative paths through the active or neutral electrode to earth ground it is called current leakage [21]. The leaked HF current can cause unwanted burns or injuries to the operator, staff or patient. It is difficult to avoid leakage, but through insulation and feedback control the leakage can be minimized.

In monopolar surgery the dispersive pad can detach, causing high current density points or that the patient is grounded at a different point than the pad—severe burns can be the result [7] [9] [25]. To prevent this, the dispersive pad is often split, introducing by its very nature an impedance between the two-lead patient return cable [21]. The ESU trips at impedance thresholds typically above $200\,\Omega$ or below $5\,\Omega$ [26] to prevent burns from the detachment.

III. Methods

For each ESU a Property Test and a Thermal Camera Test were made to find parameters of monopolar electrosurgery that can determine critical design requirements. Every test was repeated three times using randomization across all cases. First the three devices that were chosen are introduced.

TABLE I: Introduction and comparison of the ESUs selected.

Electrosurgical Unit	RDE Electrocut 100	Valleylab Force Fxc	ERBE ICC 300
Picture			
Device Class	Low-end	High-end	High-end
Estimated Price	>€600*	>€15 000**	>€15 000**
Power Range Cut	$0 - 70\,\mathrm{W}$	$0 - 120\,\mathrm{W}$	$0 - 120\,\mathrm{W}$
Power Range Coagulation	$0 - 110\,\mathrm{W}$	$0 - 300\,\mathrm{W}$	$0 - 300\,\mathrm{W}$
Mass	$2.7\,\mathrm{kg}$	$8.2\,\mathrm{kg}$	$10.2\,\mathrm{kg}$
Dimensions	10x25x18 cm	12.5x36x46 cm	15x41x37 cm
Bipolar	✓	✓	✓
Monopolar	✓	✓	✓
Ports	1	2	2
Operating Temperature	$5 - 35°\mathrm{C}$	$10 - 40°\mathrm{C}$	$10 - 40°\mathrm{C}$
Operating Humidity	$20 - 80\,\%$	$30 - 75\,\%$	$30 - 75\,\%$
REM plate	single	split	single/split

* Source: TU Delft
** Source: Jeroen Bosch Ziekenhuis

The experiments were conducted with three ESUs (see Table I). The *ERBE ICC 300* (ERBE) and *Valleylab Force FXc* (Valleylab) are regarded as high-end devices due to their wide use in hospitals of high income countries[2] (HICs), their apparent quality and large number of settings. The *RDE Electrocut 100* (RDE) is regarded as a low-end device due to its low price, simplified design and analogue controls.[3]

All three devices have various sub-settings for both monopolar coagulation and monopolar cut modes as shown in Figure B.1 (pg. 25) and Table B.1 (pg. 24). For each ESU one setting for cut mode and one setting for the coagulation mode were selected for the experiments. By measuring the waveform, current level and V_{pp}, the settings were compared to each other and the most similar were selected (for a more detailed report see Appendix B, pg. 24). In Table II the chosen ESU settings are depicted.

TABLE II: Monopolar ESU settings chosen for experiments

Device	Setting	(Mode)
RDE Electrocut 100	Normal	(Coagulation)
	Normal	(Cut)
Valleylab Force FXc	Fulgurate	(Coagulation)
	Pure	(Cut)
ERBE ICC 300	Forced	(Coagulation)
	1	(Cut)

By adjusting the power level on an ESU, the resultant tissue burn intensity can be controlled. For the ERBE and Valleylab

[2]As per Jeroen Bosch Ziekenhuis and medical device expert: Prof. J.Dankelman

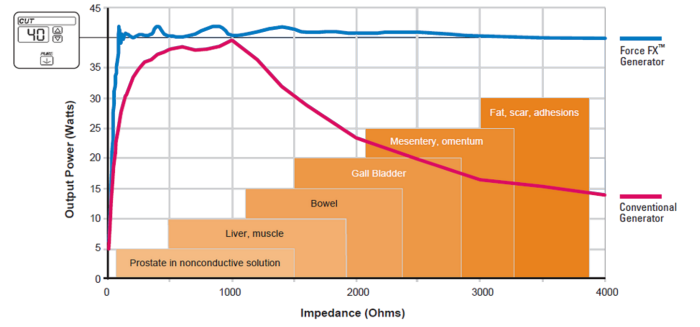[3]All three devices were chosen due to their availability in the MISIT laboratory at TU Delft.

Fig. 4: Image by Valleylab manual [27], claiming that they have—through their Instant Responce Technolog—a steady power output at 40 W over load in comparison to other conventional devices for the *Valleylab Force FXc*.

the user selects a wattage to indicate the power level, while RDE has a dimensionless scale between 1–10, where 10 is the maximum.

High-end devices often use a technology preventing a power drop over an increasing load such as ERBEs Automatic Power Control and Valleylabs Instant Response Technology (IRT). Valleylab provides a Figure (see Figure 4) showing that the IRT prevents the power to drop for loads up to $4000\,\Omega$ [27] when compared to conventional devices. The RDE does not have such a support technology.

A. Property Test

The *FLUKE QA_ES II Electrosurgical Analyzer* (FLUKE Analyzer)[4] was used to test the properties of each ESU at different power settings and with various loads between the active and neutral electrodes. The data recorded at each test were the (1) actual power ($\pm5\%$ error of reading)[5], (2) RMS current ($\pm2\%$ error of reading), (3) V_{pp} ($\pm10\%$ error of reading), (4) crest factor, and (5) voltage oscilloscope reading. The pilot tests for the Property Test can be found in Appendix C (pg. 26) and the protocol can be found in Appendix D (pg. 33). The data was used to find the following four ESU behaviours.

1) Set Power vs Real Power

The set power selected on each ESU was measured against the real power produced at a rated load of $200\,\Omega$. The real power was measured across the entire power range of each ESU at cut and coagulation modes (see the power ranges in Table I).

2) Waveform Shapes (Voltage vs Time)

The cut and coagulation waveforms were recorded using the FLUKE Analyzers integrated oscilloscope, the *Picoscope measuring meter*[6] and *Picoscope 6* software. The waveforms

[4]This device was made available thanks to the curtesy of Jeroen Bosch Hospital

[5]All errors were taken from the manual of the FLUKE *QA_ES II Electrosurgical Analyzer*. Prior to the experiments FLUKE calibrated the device. Furthermore, in a separate test the errors were verified by testing for repeatability in the pilot study (See Appendix C-B on pg. 27)

[6]This device was made available thanks to TU Delft MISIT Lab.

were tested and analysed across different loads (ΔL) over a fixed power with the following value combinations:

$$S_{Load}^{coag} = \begin{bmatrix} 40\,\text{W} \\ 70\,\text{W} \end{bmatrix} [25, 100, 200, 500, 900, 1700, 3300, 5200]\,\Omega$$

$$S_{Load}^{cut} = \begin{bmatrix} 40\,\text{W} \\ 110\,\text{W} \end{bmatrix} [25, 100, 200, 500, 900, 1700, 3300, 5200]\,\Omega$$

Furthermore, the waveforms were tested and analysed in 10 power steps ranging from the zero to the maximum power (P_{max}) of each ESU over a fixed load (ΔP):

$$S_{Power} = 200\,\Omega \cdot [0 : \frac{10}{\text{P}_{\max}} : \text{P}_{\max}]\,\text{W}$$

The RDE having a $P_{max}^{coag} = 70\,\text{W}$ and $P_{max}^{cut} = 110\,\text{W}$, and with the ERBE and the Valleylab having a $P_{max}^{coag} = 120\,\text{W}$, RDE $P_{max}^{cut} = 300\,\text{W}$.

Since the oscilloscope gave the readings with a dimensionless voltage reading, the output had to be scaled with the true V_{pp} values. For this the V_{pp} was measured, using the FLUKE Analyzer, at the same settings and scaled into the oscilloscope readings.

The data was used to analyse (1) the shape of coagulation and cut waveforms of the three ESUs and (2) how the ESUs adapt the amplitude, period and duty cycle of their waveform with a (ΔP) and (ΔL).

3) Power drop (Real Power vs Load)

To compare how the real power drops over an increasing load, the power was measured at different loads ranging from $25\,\Omega$ to $5200\,\Omega$ (See sequence in Appendix C-D (pg. 31)). For each device this test was done at maximum power ($P_{m}ax$) and $40\,\text{W}$, with $40\,\text{W}$ being a commonly used setting in electrosurgery. To compare the rate of power drop between the three devices, the load is taken at which point the measured ESU power has dropped by 50%.

4) Current Leakage

For a measure in safety, three of the monopolar leakage tests described in IEC 601.2.2, sec. 19.101b. were conducted with the FLUKE Analyzer; namely the *unloaded active*, *unloaded neutral* and *loaded test*. The electrical circuits for the three leakage measurements are shown in Figure 5. According to the standards, none of the measured leakage tests were allowed to exceed $100\,\text{mA}$ of current flow.

An example of an *unloaded active* case would be to measure the current flow if the user had the active electrode on the ground and activated the device. Similarly the *unloaded neutral* case would measure the current flow if the neutral electrode was connected to the ground and the user activated the device.

For the third test (*loaded test*) it is assumed that a patient with a $200\,\Omega$ intrinsic load is connected to the ESU. By touching earth ground accidentally with one part of his body (operation tables are normally insulated from ground), the patient gives the current an alternative path to travel. The loaded test measures how much current flows back to earth

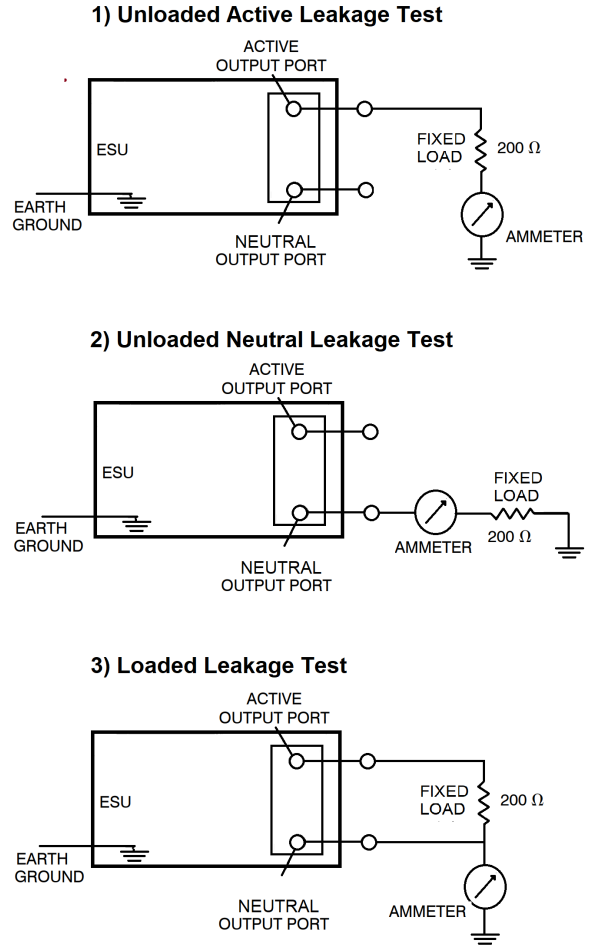ground instead of flowing back along the neutral electrode into the ESU.

Fig. 5: Three of the monopolar leakage tests described in IEC 601.2.2, sec. 19.101b. were made; namely the "unloaded active", "unloaded neutral" and "loaded test"

B. Thermal Camera Test

TABLE III: Table showing the experimental conditions chosen for the Thermal Camera Test

Variable	Description	Experimental Condition
ESUs	Different ESU models	RDE, ERBE, Valleylab
Waveform	Wave shape and length	Cut, Coagulation
Load	$L = \frac{l}{\sigma A}$	1 cm Tofu, 3 cm Tofu
Power	P=VI; intensity measure for of the heating effect	40 W/110 W (Cut) 40 W/70 W (Coagulation)

The thermal effect of the ESUs was observed through the *FLIR A35 thermal camera* on tofu samples as a tissue substitute (material selction process leading to tofu can be seen in Appendix E on pg.39) with a resolution of 60 frames
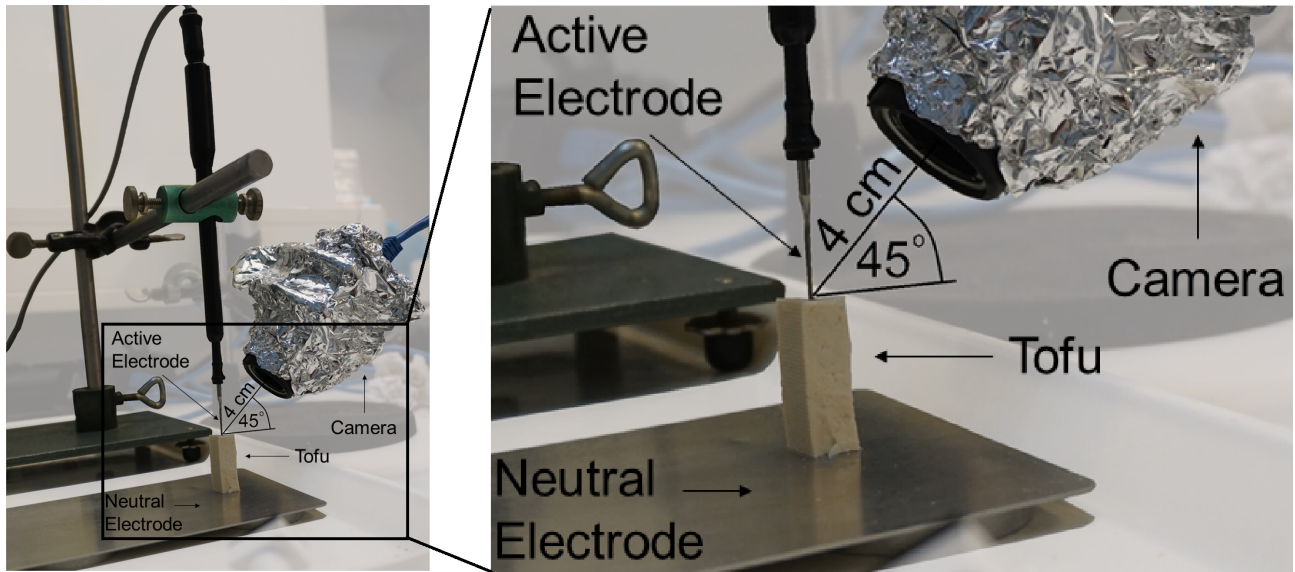
Fig. 6: Set up of the Thermal Camera Test. The camera is placed $4\,\mathrm{cm}$ from the tofu sample at an angle of $45°$. The electrode is place in the middle of the $1\,\mathrm{cm}$x$1\,\mathrm{cm}$ lateral area of the tofu sample before being activated.

a second. Using an emissivity factor of 0.96 [28] [29], the camera was pointed with a $45°$ angle at the sample (see Figure 6) to see the top (lateral) surface of the tofu sample. The tip of the $2\,\mathrm{mm}$ electrode blade was placed on the tofu, $4\,\mathrm{cm}$ from the camera lens. For safety reasons, a smoke extractor was used for the vapour [30]. To shield the camera from electromagnetic induction of the nearby electrode, the camera was wrapped in aluminium foil [31].

As variables, the coagulation and cut modes were tested at different power and load for each ESU. In Table III, all the experimental conditions can be found. Since the resistance of tofu changes with the difference in current magnitude, frequency, temperature [32] and the type of coagulant used [33] [34], an exact load was not possible to be determined (See Appemdix E (pg. 39)). Instead, the length of the tofu was changed since the resistive load L is directly proportional to length, with

$$L = \frac{l}{\sigma A}$$

where l is the length of a resistor, A is the cross-sectional area of the resistor and σ is the electrical conductivity of the resistor material. For a low and high load a tofu length of $1\,\mathrm{cm}$ and $3\,\mathrm{cm}$ was chosen respectively. These lengths were chosen through trial and error (Appendix E-C (pg. 42)) and are, for simplicity, regarded as an alternative unit of load.

With a power of $40\,\mathrm{W}$ being a common setting in operations, all settings were tested at $40\,\mathrm{W}$. Furthermore, a power of $70\,\mathrm{W}$ for coagulation and $110\,\mathrm{W}$ for cut mode were used, since these were the maximum power values of the RDE modes respectively. The ESU was activated for 2 seconds, after which the thermal camera recorded further 3 seconds of inactive cooling, having a total recording time of 5 seconds. The protocol for the Thermal Camera Test can be found in

Appendix F (pg. 44).

TABLE IV: Defining the tofu burn scale: 1 is least burnt, while 5 is severely burned

Burn Scale	1	2	3	4	5
Example Sample					

Each tofu sample tested was photographed and each thermal video was analysed and compared using Matlab. As seen in Table V, five results were then recorded for each test case. (1) The intensity of burn marks on each tofu sample was analysed using the burn scale in Table IV. Values extracted from each thermal video were (2) the maximum temperature (T_{max}), (3) the average of the maximum temperature over all time points during activation ($mean\,T_{max}$), and the area of tissue over (4) $60°\mathrm{C}$ and (5) $100°\mathrm{C}$.

To calculate the area of the thermal damage (See Figures 7a to 7d), the camera angle and the hidden thermal data behind the electrode needed to be compensated for. By knowing the width of the electrode ($2\,\mathrm{mm}$), the width of each measured pixel a could be calculated

$$a = \frac{\text{Electrode width [mm]}}{\text{Electrode width [Pixels]}} = \frac{2\,\mathrm{mm}}{19\,\mathrm{Pixels}} = 0.117\,\frac{\mathrm{mm}}{\mathrm{Pixel}}$$

Assuming that the thermal damage is symmetric around the electrode, the area of interest is determined by counting all pixels in front of the electrode ($Pxls$) (See Figure 7c) and doubling the result. to compensating for the $45°$ angle of the thermal camera, each pixel height is recalculated to be

$a/\cos(45°)$ (See Figure 7d). Therefore the total area A of the thermal damage is

$$A = 2 \cdot Pxls \cdot \frac{a^2}{\cos(45°)}$$

With the data four questions were answered:

1) How did each ESU react to changing power settings (ΔP)?

It was expected that a high power setting produced higher temperatures and larger thermal damage to the tissue when compared to a low power setting, since more energy was used. The effectiveness of the power settings in each device were explored in this question.

2) How did each ESU react to changing loads (ΔL)?

Ideally the power setting should cause the tissue to burn at the same temperature regardless of load. How well the ESUs implemented this design requirement was explored through this question.

3) How did each ESU react to changing waveform settings (Coagulation vs Cut)?

Due to the fundamental difference between the cut and coagulation waveforms, the effectiveness of each ESU wave design was explored. In this question the thermal difference of the two waveforms at the same power and load settings were compared.

4) How well did the devices produce expected values from literature?

Table V shows what resulting values should be expected when compared to literature. In this question the thermal results of each ESU were compared to the values from Table V, hence evaluating the effectiveness of the ESUs.

TABLE V: Measured variables of the Thermal Camera Test and their expected results according to literature

| SETTINGS			EXPECTED RESULTS				
Waveform	Load in tofu length	Power	Burn Scale 1-5*	T_{max} [°C]	Mean T_{max} over all time points [°C]	Area>60°C [mm²]	Area>100°C [mm²]
Cut	*Any Load*	*40 W*	1-3	*>100*	*>80*	*Smaller than Coagulation area*	
		110 W	2-3	*>120*	*>100*	N/A	
Coagulation	*Any Load*	*40 W*	2-4	*60<100*	*60<100*	*Larger than Cut area*	
		70 W	3-5	*80<120*	*80<100*	N/A	

* See Table IV for the key to the Burn Scale
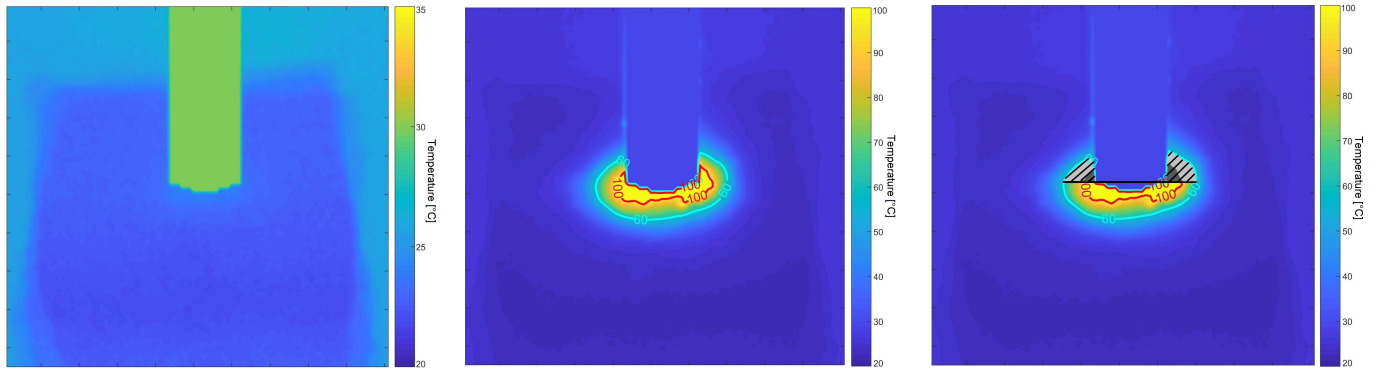
(a) Step 1: The electrode was placed on the tofu sample and were clearly seen by the camera before activation was initiated.

(b) Step 2: Once activated, the area reaching over 100°C and 60°C was determined at all time points (60 frames/s).

(c) Step 3: Since the electrode covered parts of the area of interest, the front half was selected and the pixel count was doubled.
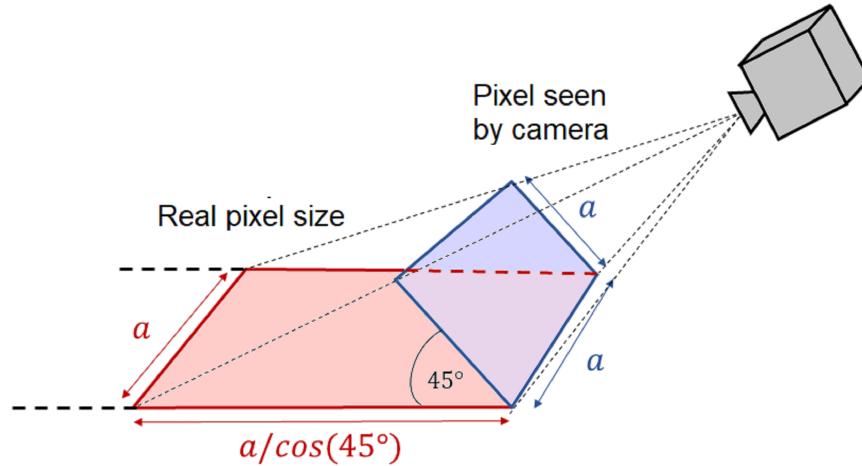
(d) Step 4: The pixels needed to be corrected for the 45° camera angle perspective.

Fig. 7: Steps to analyse each Thermal Video frame: (a) Step 1: The electrode and tofu could clearly be seen before activation was initiated. (b) Step 2: Once activated, the area reaching over 100°C and 60°C was determined at all time points (60 frames/s). (c) Step 3: Since the electrode covered parts of the area of interest, the front half was selected and the pixel count was doubled. (d) Step 4: The pixels needed compensation for the 45° camera angle.

IV. RESULTS

A. Property Test

Similar to the methods, the Property Test results were structured in four sections, describing the behaviour of the three ESUs.

1) Set Power vs Real Power
The actual power measured versus the set power selected on each of the ESUs are shown in Figures 8a-c at their set power of $200\,\Omega$. The RDE has a power knob on its interface with a dimensionless scale between 1–10, where setting 10 produced the highest power setting possible. To determine what the 1–10 RDE scale meant in wattage, the power for each setting was measured and recorded in Figure 8a. The RDEs maximum power in cut mode reached $110 \pm 4\,\mathrm{W}$ and for coagulation mode it reached $70 \pm 3\,\mathrm{W}$. The measured power increase for the RDE followed a logarithmic trajectory, where a sharp increase in power was recorded between the low settings and a low power increase was recorded between high settings.

The ERBE and the Valleylab both have a linearly increasing wattage setting on their interfaces of up to $120\,\mathrm{W}$ for the coagulation mode and $300\,\mathrm{W}$ for the cut mode (See Figures 8b and 8c). However, their actual power measured across all loads were below their set power, with the ERBE being up to 8.3% off the requested set value and the Valleylab being up to 17% off the requested set value.

2) Waveform Shapes (Voltage vs Time)
In Figure 9a-c the cut waveform shape (at $110\,\mathrm{W}$, $200\,\Omega$) showed that the Valleylab and ERBE both had, as expected for cut, a continuous sinusoidal waveform design. The RDE had an irregular sinusoidal waveform. The RDE had the lowest frequency ($f_{RDE} = 318\,\mathrm{kHz}$) and highest crest factor ($CF_{RDE} = 2.7 \pm 0.1$) while the ERBE ($f_{ERBE} = 379\,\mathrm{kHz}$; $CF_{ERBE} = 1.6 \pm 0.1$) and Valleylab ($f_{Vall} = 391\,\mathrm{kHz}$; $CF_{Vall} = 1.6 \pm 0.1$) had a higher frequency and lower crest factor reading than the RDE.

In Figure 10a-d, the coagulation waveform designs (at $70\,\mathrm{W}$, $200\,\Omega$) had a different design for each ESU. The Valleylab (Figure 10c) had the largest gap between current bursts ($34 \pm 1\,\mu s$, $n = 5$) and the highest voltage peak-to-peak readings ($V_{pp} = 975 \pm 15\,\mathrm{V}$, $n = 5$). Between the current peaks the waveform was underdamped, producing an approximate duty cycle of $DC_{Vall} \approx 40\%$. The ERBE (Figure 10d) had the smoothest curve ($12 \pm 0.5\,\mu s$, $n = 5$) between each burst of current and a voltage peak-to-peak of $V_{pp} = 900 \pm 10\,\mathrm{V}$, $n = 5$, producing the lowest duty cycle of of all ESUs ($DC_{ERBE} = 35.7 \pm 0.5\%$, $n = 5$). Compared to all ESUs, the RDE (Figure 10a) had the lowest voltage peak-to-peak ($V_{pp} = 530 \pm 60\,\mathrm{V}$, $n = 16$) with a relatively continuous waveform and a high duty cycle ($DC_{RDE} \approx 99\%$). The RDE cut waveform is similar in frequency, amplitude and CF to its coagulation waveform, which would theoretically result in no difference in tissue effect. However, when zooming out in time by 1/1000 (from μs to ms) (See Figure 10b), it can be seen that the RDE put a 25 Hz modulation over the signal (suppressing current every 10 ms) to reach the coagulating effect.

TABLE VI: With a change in power (ΔP) or load (ΔL), each ESU adapted (✓) their waveform.

Devices		Amplitude	Duty Cycle (Coagulation)	frequency (Cut)
RDE	ΔP	✓	–	–
	ΔL	✓	–	–
Valleylab	ΔP	✓	✓	–
	ΔL	✓	–	–
ERBE	ΔP	✓	✓	✓
	ΔL	✓	✓	✓

In Table VI it can be seen that the three ESUs adapted their waveforms to a change in power (ΔP) or load (ΔL) differently (refer back to Figure 1). The RDE only adapted its waveform amplitude, while the duty cycle and frequency stayed constant over an ΔP and ΔL. Also the Valleylab adapted its waveform amplitude at a ΔL. However, for a ΔP the Valleylab not only adapted its amplitude, but also its DC for the coagulation waveform. The ERBE, on the other hand, changed the DC of its waveform at coagulation mode and the frequency at cut mode with both a ΔP and ΔL.

3) Power drop (Real Power vs Load)
All three devices dropped power over an increase in load measured at a power of $40\,\mathrm{W}$ (Figure 11) as well as the maximum power (Figure 12). The measured error in the data (shown as an errorbar) stayed within the 5% error margin set by the FLUKE Analyzer (shown as the shaded area).

In general, all three devices had a low power at low voltages of $25\,\Omega$. The power then increased with a larger load, peaking between the values of $200\,\Omega$–$1700\,\Omega$ before dropping again. For both the RDE and the Valleylab, the power dropped more at the coagulation mode than their cut mode. The opposite was true for the ERBE, where the coagulation mode dropped less than the cut mode.

At the $40\,\mathrm{W}$ setting (Figure 11), the RDE (Figure 11a) had a sharp peak of power above $40\,\mathrm{W}$ (coag: $200\,\Omega$–$300\,\Omega$, cut: $300\,\Omega$–$450\,\Omega$) followed by a sharp drop in power, reaching a 50% power drop at $1700\,\Omega$ for coagulation mode and $2650\,\Omega$ for cut mode. The Valleylab (Figure 11b) held the $40\,\mathrm{W}$-level the longest compared to the other two devices (coag: $400\,\Omega$–$1200\,\Omega$, cut: $300\,\Omega$–$1700\,\Omega$) followed by a low gradient power drop. For the Valleylab the load did not cause the power to drop past 50% for both cut and coagulation mode. The ERBE (Figure 11c) had a round peak value at around $500\,\Omega$ for both the cut and coagulation mode, barely reaching the $40\,\mathrm{W}$ setting. After the peak value, the power dropped rapidly, falling to a 50% power drop at $3025\,\Omega$ for coagulation mode and $1475\,\Omega$ for cut mode.

At maximum power setting (Figure 12), the three devices also dropped power after reaching a peak value, however, the rate of power decrease was different to the $40\,\mathrm{W}$ case. The RDE (Figure 12a) dropped slower than at the $40\,\mathrm{W}$-case, falling to a 50% power drop at $3075\,\Omega$ for coagulation mode and $3700\,\Omega$ for cut mode only. These values can be compared to Valleylab (Figure 12b), which dropped the power

(a) RDE Electrocut 100 Power scale

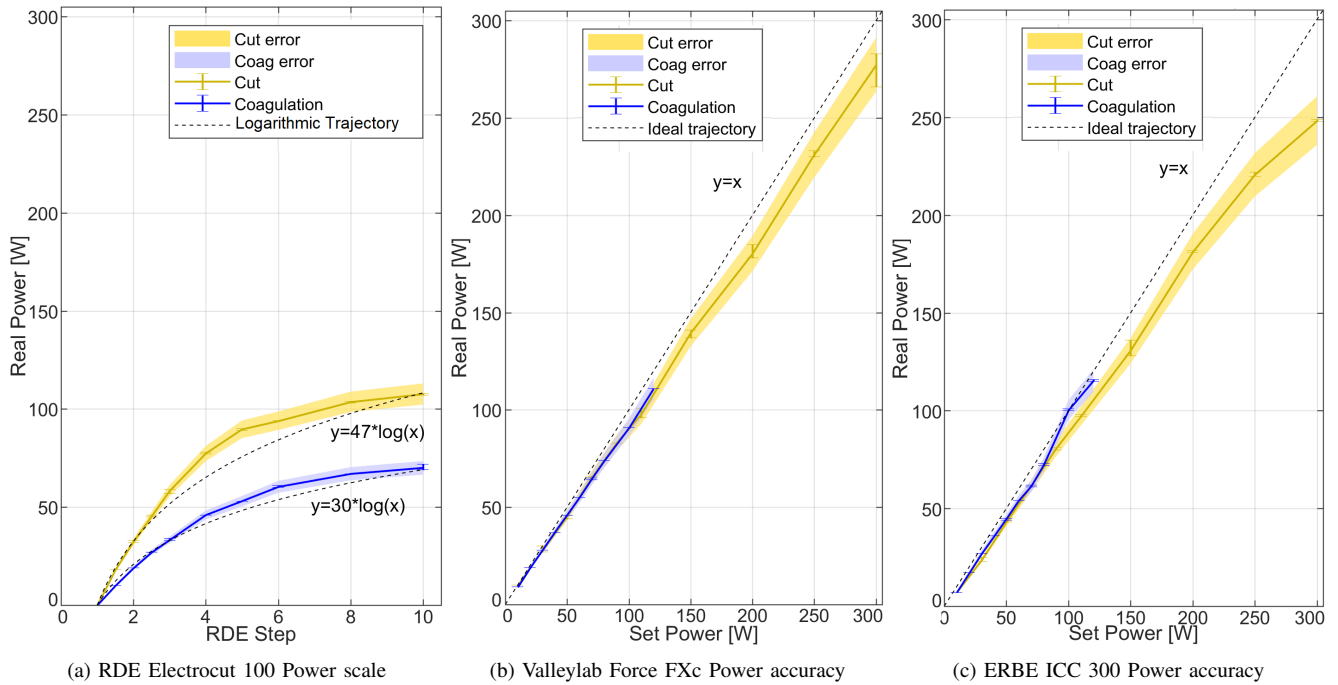(b) Valleylab Force FXc Power accuracy

(c) ERBE ICC 300 Power accuracy

Fig. 8: Set power vs real power, comparing the three ESUs.(a) The RDE had a dimensionless power scale, producing a non-linear power increase. The ERBE (b) and the Valleylab (c) had a lower actual power, than what the settings indicated on the ESU display. The intrinsic 5% error of the measuring device is shown as the shaded area and the measured errors is shown as errorbars.

to 50% with a load of $4620\,\Omega$ for coagulation mode and $2950\,\Omega$ for cut mode. The ERBE dropped a lot faster than in the $40\,\text{W}$-case, falling to a 50% power drop at $1375\,\Omega$ for coagulation mode and $390\,\Omega$ for cut mode.

4) Current Leakage

In Figures 13a-b the results of the three leakage tests for the cut mode and the coagulation mode can be seen. The loaded test simulates leakage with a patient attached to the ESU, while the unloaded test simulated leakage without a patient attached. The dotted red line indicates the $100\,\text{mA}$ limit which may not be exceeded. An error bar indicates the deviations of the measured data.

For the cut mode in Figure 13a, ERBE had the lowest leakage ($< 25\,\text{mA}$) for all three leakage tests. The RDE and Valleylab both had a high *unloaded active* leakage, with the Valleylab exceeding the $100\,\text{mA}$ leakage limit with a leakage reading of $108\,\text{mA}$. At $60\,\text{mA}$ the RDE recorded the highest leakage for the *loaded test*.

For the coagulation mode in Figure 13b none of the devices exceeded the $100\,\text{mA}$ leakage limit. Valleylab's unloaded leakage setting was the highest leakage measured with $93\,\text{mA}$. However, once a load was applied (*loaded test*), the leakage of the Valleylab dropped to a lower value ($24\,\text{mA}$) than that of the RDE ($47\,\text{mA}$) and ERBE ($48\,\text{mA}$). For all three devices, the *unloaded active* test recorded the highest leakage reading of the three tests.
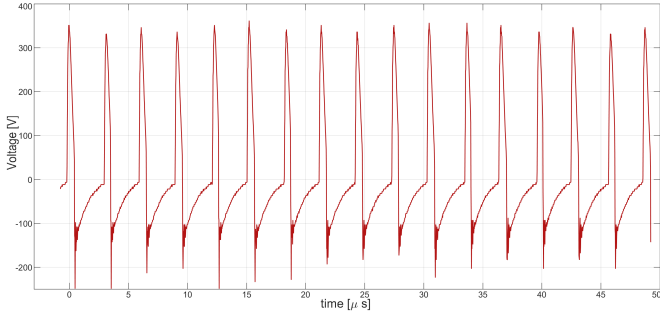
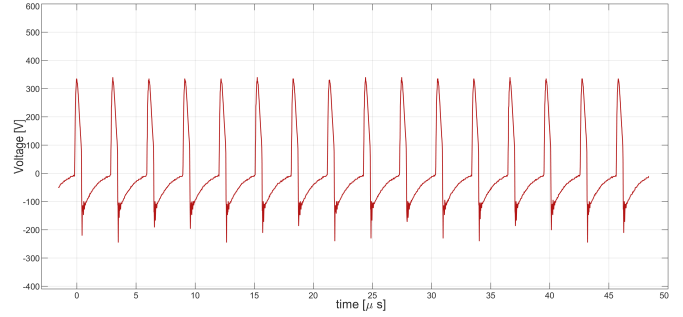(a) *RDE Electrocut 100* cut mode waveform (f $= 318$ kHz; $CF = 2.7\pm1$).
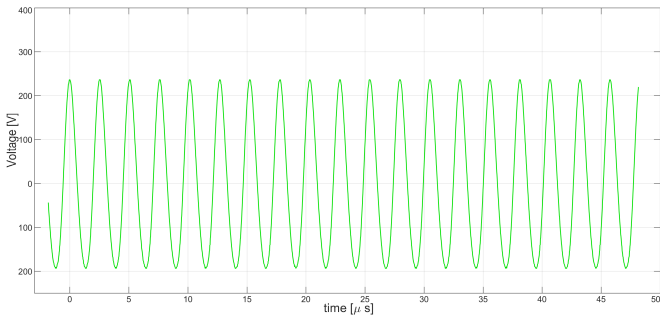
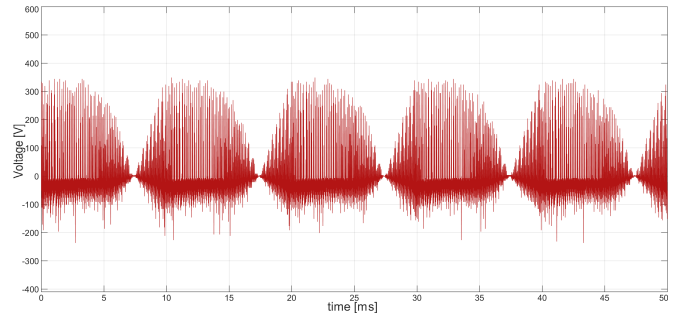(b) *Valleylab Force FXc* cut mode waveform (f $= 391$ kHz; $CF = 1.6\pm1$).
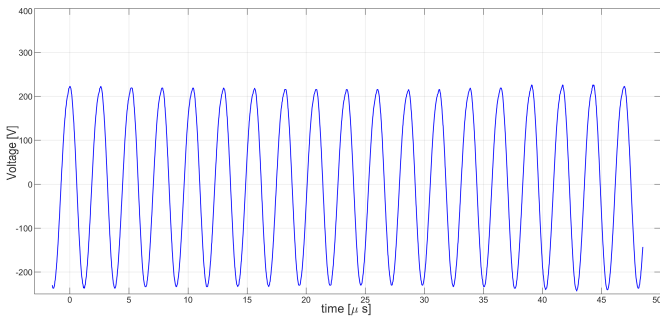
(c) *ERBE ICC 300* cut mode waveform (f $= 379$ kHz; $CF = 1.6 \pm 1$).
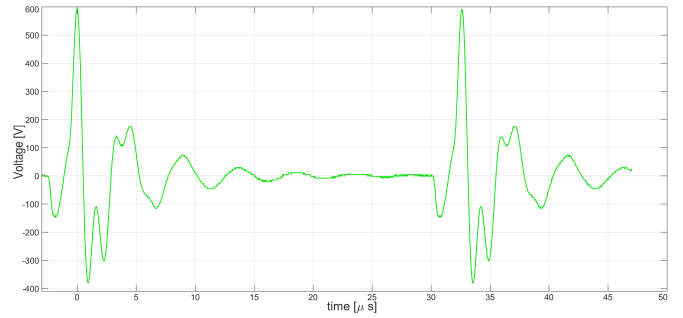
Fig. 9: Cut mode waveforms at power $= 110$ W and a rated load of $200\,\Omega$ showed that the RDE had a less smooth sinusoid than the Valleylab and ERBE.
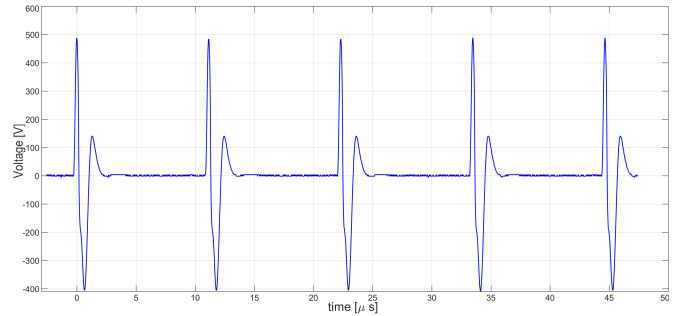

(a) *RDE Electrocut 100* coagulation mode waveform at $0 - 50\,\mu s$ (Duty Cycle$\approx 99\%$)

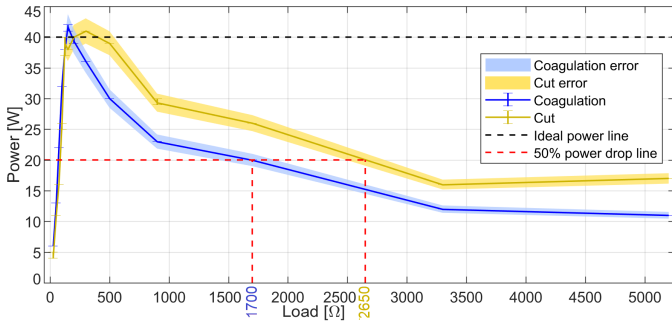(b) *RDE Electrocut 100* coagulation mode waveform at $0 - 50$ ms

(c) *Valleylab Force FXc* coagulation mode waveform (Duty Cycle$\approx 40\%$)
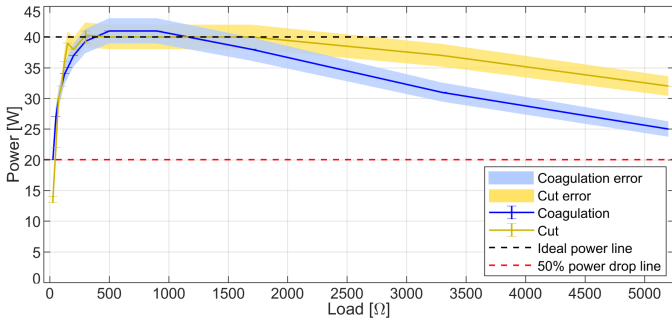

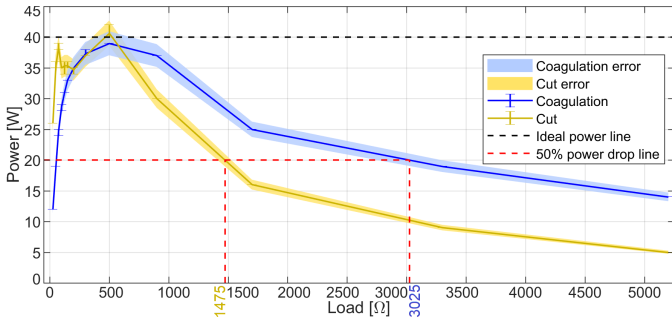(d) *ERBE ICC 300* coagulation mode waveform (Duty Cycle$= 35.7\pm0.5\%$)

Fig. 10: Coagulation mode waveforms at $power = 70$ W and a rated load of $200\,\Omega$ showed large differences between the three ESUs.

(a) *RDE Electrocut 100*
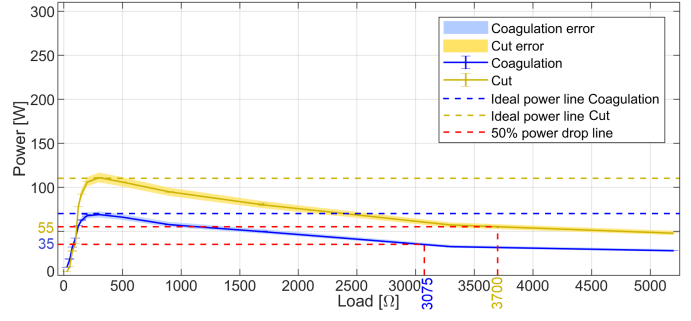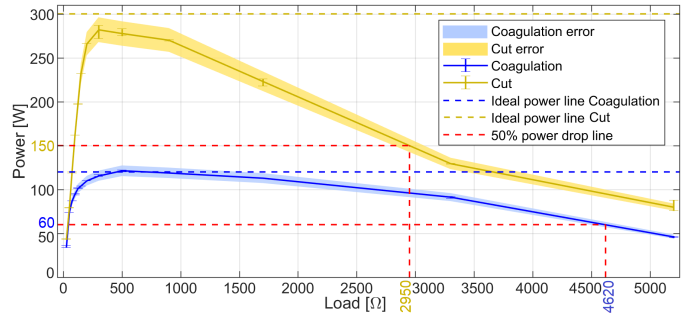
(b) *Valleylab Force FXc*
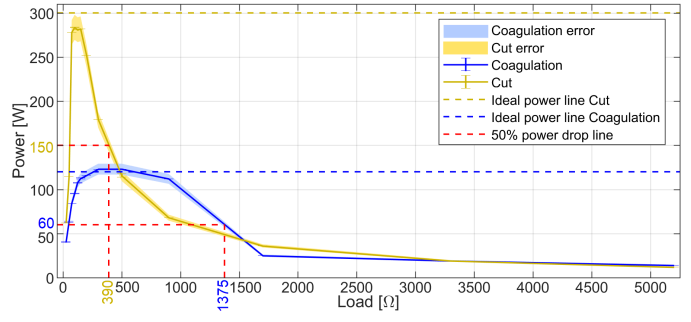
(c) *ERBE ICC 300*

Fig. 11: Figure shows a power drop over load at a power of 40 W. The intrinsic 5% error of the measuring device is shown as the shaded area and the measured errors is shown as errorbars. The red line indicates coordinates at 50% power drop.

(a) *RDE Electrocut 100*

(b) *Valleylab Force FXc*

(c) *ERBE ICC 300*

Fig. 12: The power drop over load of three ESUs set at maximum power is shown. The intrinsic 5% error of the measuring device is shown as the shaded area and the measured errors is shown as errorbars. The red line indicates coordinates at 50% power drop.
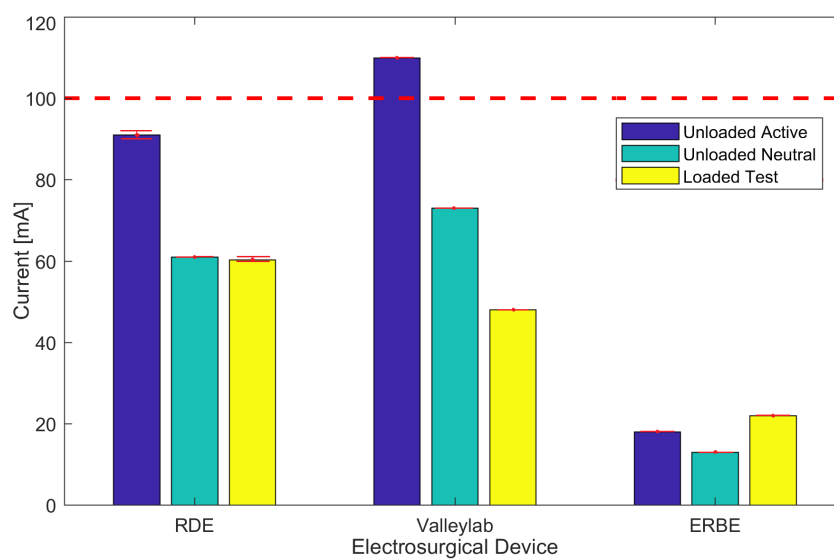
(a) Cut mode leakage
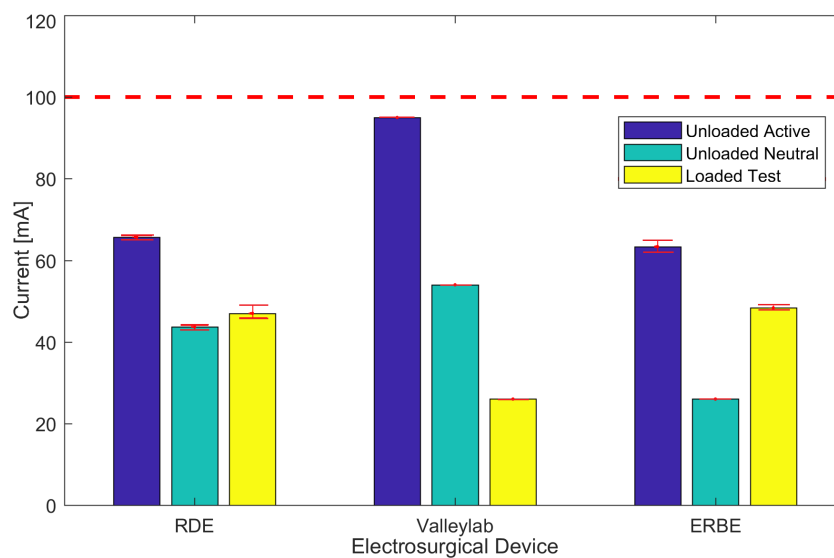
(b) Coagulation mode leakage

Fig. 13: The leakage of three ESUs was measured for both (a) the cut mode and (b) the coagulation mode. Three leakage tests were made per ESU, namely "unloaded active", "unloaded neutral" and "loaded test". Current leakage was not allowed to exceed $100 mA$ for safety reasons. The Leakage tests were made at $200\,\Omega$ and maximum power.

B. Thermal Camera Test

Table VII numerically summarized the results of the Thermal Camera Test numerically. Figure 14 is a sample taken from Appendix G-A (pg.47) (Figures G.1–G.8), showing the thermal damage and the maximum temperatures over time. Figure 14 investigates the "*Coagulation; L=1cm; P=40W*"–case for each ESU, where—over time—the area of tissue at $60°C$ and $100°C$ (in Figure 14a) and the maximum temperature (in Figure 14b) is shown.

The Valleylab and ERBE recorded high temperatures, exceeding the $177°C$ measuring threshold of the FLIR A35 Thermal Camera, limiting parts of the results. The full numerical and graphical results of the Thermal Camera Test can be found in Appendix G (pg.46). Using this data, the results were focused towards the four questions suggested in the methods.

1) How did each ESU react to a changing power setting (ΔP)?

When referring to Table VII it can be seen that with an increase in power, both the Valleylab and the RDE, had a increase in burn scale (except for RDE "*Cut; L=1cm*"–case and "*Coagulation; L=1cm*"–case), T_{max}, $mean\ T_{max}$, and the thermal damaged area>$60°C$ (except for the RDE "*Cut; L=1cm*"–case) and area>$100°C$ across all settings. However, the ERBE hardly distinguished between the power increase from $40\,W$ to $110\,W$ at cut mode and $40\,W$ to $70\,W$ at coagulation mode. For example, at the "*Cut; L=1cm*"–case, the T_{max} and $meanT_{max}$ of the ERBE hardly distinguished between the power settings, while at the "*Coagulation; L=3cm*"–case the device even became less effective at a higher power setting. The same phenomenon could be observed when looking at the thermal damage, where not more than a 7% increase in thermal damage was observed for the ERBE, even though the power nearly doubled.

Similarly, when comparing the Valleylab and RDE in Figures G.1 with G.2, G.3 with G.4, G.5 with G.6, and G.7 with G.8 (Appendix G), a higher temperature and thermal damage over activation was achieved across all settings, except for the RDE "*Cut; L=1cm*"–case (Figures G.1a & G.2a). Furthermore, the difference between the power settings were bigger for the Valleylab than the RDE for both maximum temperatures and thermal tissue damage. The ERBE again did not show a distinct difference when the power was increased in Figures G.1–G.8, showing a poor power control system.

2) How did each ESU react to a changing load (ΔL)?

In Table VII, all three devices generally showed a considerable drop in temperature at a higher $3\,cm$ tofu load in comparison to the lower $1\,cm$ tofu load—especially at coagulation mode.

The Valleylab stayed the most consistent for the tofu burn scale and temperatures T_{max} and $meanT_{max}$ when comparing it to the other two ESUs. At $40\,W$ and $3\,cm$, the RDE dropped to $mean\ T_{max}$ values below $60°C$ (cut dropped from mean temperatures of $82.2°C$–$55.2°C$ and coagulation from $72.9°C$–$49.3°C$), indicating that no effective thermal damage

was made. At coagulation, the ERBE had a drop of T_{max} by $\pm73°C$ at $40\,W$ and $\pm94°C$ at $70\,W$, which was the highest temperature drop when compared to the other two ESUs.

Similarly, when comparing Figures G.1 with G.3 and G.2 with G.4 (cut mode) the load increase had a lower impact on the temperature and thermal damage than when comparing Figures G.5 with G.7 and G.6 with G.8 (coagulation mode). At low loads, the maximum temperature quickly reached a constant temperature platform (Figures G.1b, G.2b, G.5b, G.6b) during activation. At high loads (Figures G.3b, G.4b, G.7b, G.8b) and $40\,W$, the temperature platform was often only reached, if at all, after 1 second of activation only. Higher power settings reduced this lag.

3) How did each ESU react to a changing waveform setting (Coagulation vs Cut)?

In Table VII, the RDE showed only a slight increase in $meanT_{max}$ for the cut waveform in comparison to the coagulation waveform of between 2.3–$19.8°C$. Valleylab (>$67°C$) and ERBE (>$77°C$), on the other hand, showed a steep increase in $meanT_{max}$ from cut mode to coagulation mode at a low load of $1\,cm$. At a high load of $3\,cm$, the Valleylab also recorded large $meanT_{max}$ gaps between coagulation and cut (>$40.8°C$), however, ERBE doesn't (<$8.4°C$).

Similarly, when comparing Figures G.1 with G.5 and G.2 with G.6 for the low load of L=1cm and when comparing G.3 with G.7 and G.4 with G.8 for the high load of L=3cm, Valleylab shows the most distinct temperature differences between the waveforms. Higher temperatures are reached and larger thermal damage is caused for the cut mode. At low loads, the ERBE also distinguished thermally between the waveforms considerably, however at high loads the waveforms distinguished much less. In comparison to the ERBE and the Valleylab, the RDE seems to have similar temperature and thermal damage trajectories between the cut mode and coagulation mode, making them hard to distinguish.

For all devices (most distinct with the Valleylab), the thermal damage trajectory (Figures G.1a–G.4a) peaks in the beginning of activation for the cut mode. However, for the coagulation mode (Figures G.5a–G.8a), the peak is more to the back of the activation.

4) How well did the devices produce expected values from literature?

Table VIII shows how many of the measured thermal values from Table VII fell into the expected frame described in Figure V. Valleylab performed best with 22/32 values correct, while the RDE had the least correct values with 13/32. The ERBE also performed poorly with 16/32 values falling into the expected value bracket.

The RDE often did not reach thermal values hot enough to damage tissue, missing some target values for T_{max} and $mean\ T_{max}$. Furthermore, when comparing the thermal damage caused, the cut mode caused larger tissue damage than the coagulation mode, which was not in line with the expected values.

The Valleylab kept most values in the expected results bracket, except for T_{max} and $meanT_{max}$ in coagulation mode.
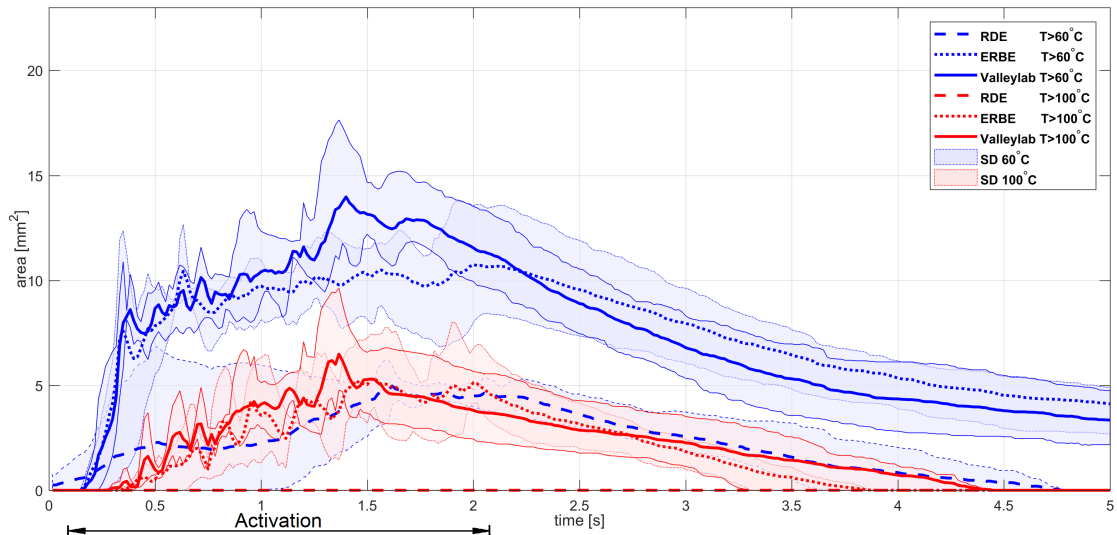
(a) Area of Thermal damage above 60°C (blue) and 100°C (red) respectively over time.
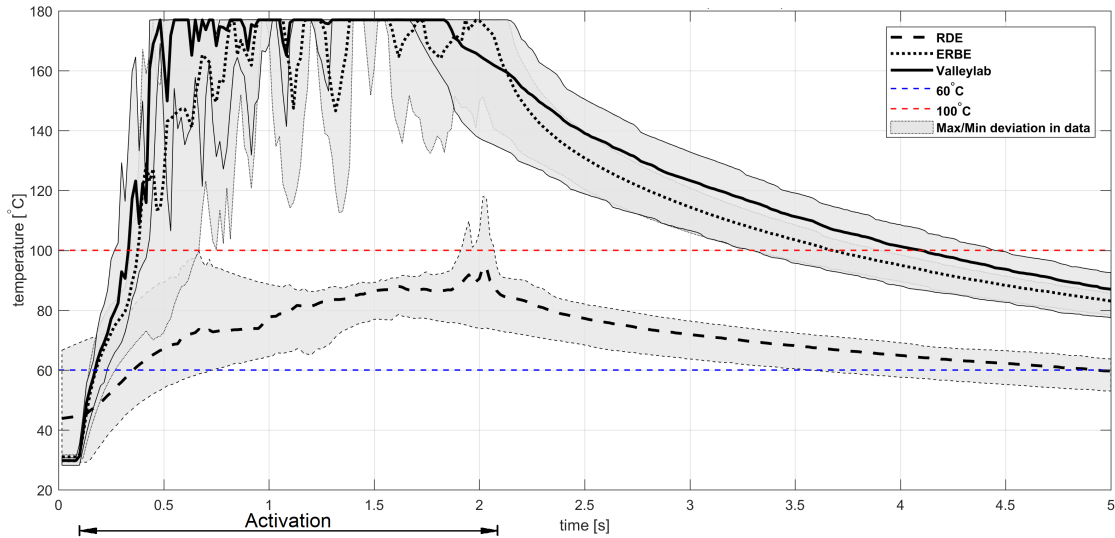
(b) Maximum temperature measured over time.

Fig. 14: Sample from the results (Settings: *Coagulation, Tofu=1cm; P=40W*). Between 0.1 s–2.1 s is activation followed by 3 s of cooling. (a) Thermally damaged area was measured. The blue lines indicate the surface area on tofu over 60°C over time, causing permanent cell dessication and protein denaturation (used in coagulating mode). Red indicates the surface area over 100°C over time, causing vaporisation of tissue (Used in cut mode). (b) Maximum Temperature measurement over time. At over 60°C coagulation occurs. At over 100°C vaporization occurs. The thermal camera limited the temperature measurements to 177°C. For similar graphics see Figures G.1–G.8 in Appendix G-A

Temperatures were reached that were much higher than what was expected for coagulation.

The ERBE had mostly a larger thermal area for coagulation mode than for cut mode, which adhered to the expected value range. However, the T_{max} and $mean\ T_{max}$ were either too low to cut tissue or too high to coagulate tissue.

In summary, the ERBE showed little measurement changes with an increased power setting, unlike the large thermal damage and temperature increases of the Valleylab and the RDE. At an increased load all three devices indicated a drop in performance, however, RDE and ERBE struggle the most. When changing between cut mode and coagulation mode, RDE showed little change in thermal results, while Valleylab and ERBE had a notable increase in temperature at low loads. Valleylab produced the most expected values, while RDE produced the least.

TABLE VII: Test data comparing the thermal reactions of three electrosurgical devices on tofu

	SETTINGS				RESULTS			
	Waveform	**Tofu Length Load×Length**	**Power**	**Burn Scale 1-5***	**T_{max} [°C]**	**Mean T_{max} over all time points [°C]**	**Area>60°C [mm²]**	**Area>100°C [mm²]**
Expected Result	*Cut*	*Any Load*	*40 W*	*1-3*	*>100*	*>80*	*Smaller than Coagulation area*	
			110 W	*2-3*	*>120*	*>100*		
	Coagulation	*Any Load*	*40 W*	*2-4*	*60<100*	*60<100*	*Larger than Cut area*	
			70 W	*3-5*	*80<120*	*80<100*		
RDE Electrocut 100	Cut	1 cm	40 W	2	$101^{+4.10}_{-5.78}$	$82.2^{+2.39}_{-2.29}$	8.18 (±2.31)	0.018(±0.002)
			110 W	2	$139^{+37.8}_{-21.2}$	$101^{+17.8}_{-12.6}$	5.15 (±0.902)	0.161(±0.033)
		3 cm	40 W	1	$66.7^{+15.3}_{-8.36}$	$55.2^{+13.7}_{-7.78}$	3.16 (±1.12)	0.00 (±0.00)
			110 W	2	$164^{+12.5}_{-8.49}$	$96.2^{+14.3}_{-10.9}$	7.62 (±2.00)	0.152(±0.029)
	Coagulation	1 cm	40 W	2	$103^{+14.9}_{-11.7}$	$75.9^{+7.97}_{-7.18}$	4.97 (±1.32)	0.00 (±0.00)
			70 W	2	$122^{+5.64}_{-3.82}$	$95.9^{+3.44}_{-2.14}$	7.93 (±1.46)	0.116(±0.019)
		3 cm	40 W	1	$59.3^{+9.19}_{-10.7}$	$49.3^{+9.76}_{-7.63}$	1.89 (±0.67)	0.00 (±0.00)
			70 W	2	$101^{+7.33}_{-12.4}$	$76.4^{+8.14}_{-14.8}$	12.0 (±4.45)	0.027(±0.006)
Valleylab Force FXc	Cut	1 cm	40 W	2	$126^{+27.6}_{-20.3}$	$89.3^{+5.39}_{-2.88}$	6.61 (±1.45)	0.089(±0.020)
			110 W	4	$>177^{+0.00}_{-0.00}$	$>135^{+35.1}_{-26.3}$	12.4 (±2.09)	4.92 (±0.911)
		3 cm	40 W	2	$103^{+9.62}_{-7.64}$	$79.2^{+2.92}_{-2.81}$	8.54 (±2.58)	0.018(±0.003)
			110 W	4	$>177^{+0.00}_{-0.00}$	$>155^{+10.2}_{-19.7}$	9.09 (±1.74)	3.76 (±0.828)
	Coagulation	1 cm	40 W	4	$>177^{+0.00}_{-0.00}$	$>157^{+4.49}_{-4.52}$	14.0 (±2.65)	6.49 (±1.83)
			70 W	5	$>177^{+0.00}_{-0.00}$	$>170^{+1.19}_{-1.81}$	20.3 (±4.76)	9.21 (±2.49)
		3 cm	40 W	3	$>177^{+0.00}_{-0.00}$	$>120^{+9.87}_{-18.2}$	9.52 (±3.41)	3.53 (±1.14)
			70 W	4	$>177^{+0.00}_{-0.00}$	$>154^{+5.77}_{-10.1}$	12.0 (±3.32)	5.26 (±1.60)
ERBE ICC 300	Cut	1 cm	40 W	2	$94.4^{+4.75}_{-4.65}$	$84.4^{+5.60}_{-7.28}$	6.96 (±1.39)	0.00 (±0.00)
			110 W	2	$94.8^{+2.51}_{-2.36}$	$86.1^{+2.17}_{-2.63}$	7.10 (±1.23)	0.00 (±0.00)
		3 cm	40 W	1	$81.8^{+8.02}_{-12.0}$	$64.8^{+6.07}_{-7.35}$	7.23 (±2.67)	0.00 (±0.00)
			110 W	1	$93.8^{+8.85}_{-7.64}$	$73.2^{+8.89}_{-10.86}$	8.33 (±3.05)	0.00 (±0.00)
	Coagulation	1 cm	40 W	4	$>177^{+0.00}_{-0.00}$	$>149^{+6.76}_{-11.8}$	10.8 (±2.88)	5.33 (±1.87)
			70 W	4	$>177^{+0.00}_{-0.00}$	$>163^{+4.28}_{-5.58}$	11.5 (±2.59)	5.38 (±1.51)
		3 cm	40 W	2	$104^{+70.8}_{-51.8}$	$65.3^{+22.1}_{-20.87}$	6.25 (±2.39)	0.787(±0.188)
			70 W	3	$80.9^{+9.90}_{-15.4}$	$64.8^{+7.37}_{-9.89}$	4.59 (±1.63)	0.00 (±0.00)

* See Table IV for the key to the Burn Scale

The table compares the thermal reaction of three electrosurgical devices on tofu. Thermal tests using a thermal camera were made to compare the waveform, resistive load and power settings. The results were divided into 5 categories. First, the burn scale (defined in Table IV) indicates the physical appearance of the tofu after each test. Second, T_{max} indicates the absolute maximum value measured during each test. Third, the mean of all maximum temperatures over activation (mean T_{max}) was measured. Lastly, the area of thermal damage over $60^{circ}C$ and $100^{circ}C$ was measured. How these results compare to the expected values of each setting can be seen in Table VIII. Temperatures of $177^{circ}C$ were the upper limit of the *FLIR A35* thermal camera. For all results that measured a value of over $177^{circ}C$, the value was given a greater-than symbol (>)

TABLE VIII: Test data comparing three electrosurgical devices.

	SETTINGS				RESULTS				TOTAL
	Waveform	**Tofu Length** Load∝Length	**Power**	**Burn Scale 1–5***	T_{max} [°C]	**Mean T_{max} over all time points [°C]**	**Area>60°C [mm²]**	**Area>100°C [mm²]**	Sum of expected true values
Expected Result	*Cut*	*Any Load*	*40 W*	*1-3*	*>100*	*>100*	*Smaller than Coagulation area*	*Smaller than Coagulation area*	32 (✓)
			110 W	*2-3*	*>120*	*>100*	*N/A*		
	Coagulation	*Any Load*	*40 W*	*2-4*	*60<120*	*60<100*	*Larger than Cut area*	*Larger than Cut area*	
			70 W	*3-5*	*80<120*	*60<100*	*N/A*		
RDE Electrocut 100	**Cut**	**1 cm**	**40 W**	2 (✓)	✓	✓	✗	✗	13/32 (✓)
			110 W	2 (✓)	✓	✓	–	–	
		3 cm	**40 W**	1 (✓)	✗	✗	✗	– (Same value)	
			110 W	2 (✓)	✓	✗	–	–	
	Coagulation	**1 cm**	**40 W**	2 (✓)	✗	✓	✗	✗	
			70 W	2 (✗)	✗	✓	–	–	
		3 cm	**40 W**	1 (✗)	✗	✗	✗	– (same value)	
			70 W	2 (✗)	✓	✗	–	–	
Valleylab Force FXc	**Cut**	**1 cm**	**40 W**	2 (✓)	✓	✓	✓	✓	22/32 (✓)
			110 W	4 (✗)	✓	✓	–	–	
		3 cm	**40 W**	2 (✓)	✓	✗	✓	✓	
			110 W	4 (✓)	✓	✓	–	–	
	Coagulation	**1 cm**	**40 W**	4 (✓)	✗	✗	✓	✓	
			70 W	5 (✓)	✗	✗	–	–	
		3 cm	**40 W**	3 (✓)	✗	✗	✓	✓	
			70 W	4 (✓)	✗	✗	–	–	
ERBE ICC 300	**Cut**	**1 cm**	**40 W**	2 (✓)	✗	✗	✓	✓	16/32 (✓)
			110 W	2 (✓)	✗	✗	–	–	
		3 cm	**40 W**	1 (✓)	✗	✗	✗	✓	
			110 W	1 (✗)	✗	✗	–	–	
	Coagulation	**1 cm**	**40 W**	4 (✓)	✗	✗	✓	✓	
			70 W	4 (✓)	✗	✗	–	–	
		3 cm	**40 W**	2 (✓)	✗	✓	✗	✓	
			70 W	3 (✓)	✓	✗	–	–	

* See Table IV for the key to the Burn Scale

The table compares the thermal reaction of three electrosurgical devices on tofu. Using the results described in Table VII, each value was compared to the expected value. An "✓" indicates that the result correlates with the expected value. "✗" indicates that the result do not correlate with the expected value. For the thermal damage tests (Area > 60°C, Area > 100°C), a power of 110W and 70W cannot be compared and are therefore not applicable.

V. Discussion

From current high-and low-end devices, critical design parameters were found that are important to consider for an ESU in a LMICs setting. Using the Property Test, different design parameters were found. Through the Thermal Camera Test, many of these design parameters could be tested on their thermal effectiveness. The design parameters were then analysed and evaluated to find design requirements indicating how robust, transportable, effective, affordable, sterilisable and safe a new ESU in a LMIC would have to be.

A. Critical design requirements

A simple user interface with an easy power control is important for the management of an ESU. For the power control, the RDE showed a linearly increasing power setting, while the ERBE and Valleylab had a power setting displaying the wattage. As the results showed, the wattage varied considerably with different tissue loads, making a wattage display meaningless. Furthermore, it is also expected that wattage for a surgeon does not have a clinical meaning, since it is not his field of expertise, making an wattage display unnecessary.

Unlike the linear power increase of the Valleylab and ERBE, the RDE had a logarithmic increase in power for the power setting. This high increase in power between low settings and the low increase in power at high settings is counter-intuitive and should be avoided. Furthermore, an analogue control (e.g. RDE) is robust and can be repaired by a local electrician if necessary. Therefore, a simple linear and dimensionless power control in an analogue interface environment is suggested for the user interface.

Within the range of tissue impedance, the output power should vary as little as possible between high and low loads. However, all three ESUs indicated a drop in power with an increasing load. The RDE and the ERBE had a large power drop, while the Valleylab had a relatively stable power control.[7] This shows that Valleylabs Instant Response Technology is effective and that ERBEs Automatic Power Control is ineffective. A power control system is useful for a surgeon, since he can predict what tissue effect to expect, no matter the tissue load. However, this technology could increase the price of an ESU.

A clean waveform helps to distinguish between the cutting vaporization effects expected for the cut mode and the tissue denaturation expected for the coagulation mode. Furthermore, clear sinusoidal waveforms helps the ions and particles in the cell to be attracted by the changing polarity of the AC current, efficiently heating the tissue through the high frequency vibrations. In the Thermal Camera Test results the RDE showed little thermal differences between cut and coagulation waveforms, while ERBE and Valleylab had a notable difference. Therefore, the surgeon would not see a

large difference between choosing the cut and coagulation setting for the RDE, making this an ineffective mode selection. This finding shows that the RDEs modular suppression of its irregular sinusoidal waveform in coagulation (Figure 10b) performs poorly. Therefore, a clean sinusoidal waveform for the cut mode and a clear duty cycle for coagulation mode are suggested to differentiate the two.

It is expected, that the three ESUs have a similar thermal output when exposed to the same waveform, power and load. However, at constant power the RDE measured much lower thermal tissue damage and temperatures than the ERBE and the Valleylab. The lack of temperature generation can be attributed to the poor waveform quality of the RDE, which has a long positive voltage peak and a short negative voltage peak. Due to the pulse like peaks, the RMS voltage is much lower than the peak voltage, reducing the effective power. This indicates once again that the waveform design of RDE is less effective than that of ERBE and Valleylab in terms of both cut and coagulation. With the previous point emphasizing the importance to differentiate cut and coagulation mode, it is now also emphasized that sinusoidal waveforms with clear positive and negative polarities are suggested with as little noise as possible.

In an effort for a quality performance, the ESUs adapted their waveforms to a ΔP or ΔL (Table VI): ERBE changed its amplitude, duty cycle and frequency; Valleylab adapted its amplitude and duty cycle; and the RDE only adapted its waveform amplitude. When analysing the thermal performance of these ESUs, it would be intuitive that more changes to the waveform would produce clear thermal output. However, with a power increase, the ERBE showed a poor temperature rise in comparison with the RDE and the Valleylab. Similarly with a high load, the ERBE showed the steepest power drop together with the RDE. This shows that a ΔP and ΔL adaption of the duty cycle and frequency can be ineffective and possible even counter-productive. Therefore, a power control system does not necessarily need to adapt the duty cycle and frequency with an increasing ΔP and ΔL; an amplitude change could be effective enough.

As it was shown in Table VIII, the Valleylab was accurate in achieving expected thermal values in comparison to the ERBE and RDE, showing the high quality of the device. While the Valleylab and ERBE sometimes reached temperatures that were too high, the RDE was often missing the high power levels to reach the required temperatures to cut or coagulate tissue. A power setting larger than RDEs maximum power settings of 70 W for the coagulation mode and 110 W for the cut mode are therefore suggested if choosing RDEs waveform. This would give the device more possibilities in treating tissue at higher impedances.

When regarding the physical properties of the ESUs, the RDE is the most transportable and manoeuvrable due to its light weight and small size. Unlike the ERBE and Valleylab, the RDE also has a handle to pick it up easily. This design is practical in a LMICs giving mobility to the surgeon. A light weight, small size and a handle are therefore suggested.

---

[7]However, Valleylab is still very far off from what they claim in Figure 4 when compared to Figure 11. Valleylab wrongly denies any power drop up to a load of $4000\,\Omega$.

Since split neutral electrodes have been introduced to electrosurgical devices, virtually all burns involving the neutral electrode have been eliminated [10]. Since the RDE only has the capability to use a single plated electrode, unlike the ERBE and Valleylab, this can cause unwanted safety issues. Therefore a split return electrode is suggested, which allows for the ESU to trip, once the return electrode pad comes off.

The RDE comes with reusable and sterilisable cables as well as an active and a neutral electrodes. Furthermore, much of the RDE hardware, such as the plugs are universal, enabling easy access to spare parts making local maintenance possible. For a LMIC setting this is good, since this independence from the producer is key for mobility and independence of the medical manufacturer [4].

B. Experimental Improvements

Even though clear data was mostly obtained throughout the experiments, improvement to data and experimental set-ups can be made in hindsight. The three electrosurgical devices that were compared gave some significant information about current ESU models, however, there are hundreds of different ESU models on the market. A larger pool of ESUs could improve findings and potentially give a better insight into technical and safety designs.

In the Property Test the FLUKE Analyzer was able to measure many important parameters, but two missing essential measuring parameters were identified. First, a measure of the stability of the signal over time would have given an insight into the precision of the ESUs outputs. For example, if an ESU was activated for 5 seconds, it can be determined how consistent the output would be throughout this time period. Second, an AC leakage test could not be made, which is a measurement of the AC input line current leakage from the chassis and patient connected probes to earth ground respectively [21]. Unlike HF leakage, the purpose is to insure that the patient, user or staff do not experience low frequency electric shock.

For the Thermal Camera Test, clear results were observed, however, the following four factors could improved the results. First, the FLIR A35 thermal camera does not record temperatures higher than $177°C$. This influenced the data at high power, since it pulled down T_{max} and $mean\ T_{max}$. However, only temperatures above 100 degrees were significant to make conclusions, making temperature measurements over $177°C$ less relevant. Furthermore, the FLIR A35 was an uncooled thermal camera. A cooled thermal camera uses photon sensors, increasing sensitivity, frame rate and temperature range of the recording [26]. By using a cooled camera clearer temperature bursts and a higher resolution would result in more detailed data collection.

Second, the Thermal Camera Test only looked at the surface area of thermal tissue damage and not the volume and depth of temperature penetration. This would show how much thermal damage occurs that cannot be seen with the naked eye, hiding important information for the surgeon [8], [35]. It is also predicted that the three ESUs vary in thermal penetration depth due to their property designs (e.g. waveform design).

Measuring inside of the tissue would be complicated and time consuming to achieve, however, it has been attempted before with thermistors [8].

Third, the tofu samples taken in the Thermal Camera test had a cross-sectional surface area of $1\,cm$ x $1\,cm$. During the data processing it was observed that the sides of the samples cooled the thermal area, preventing it to expand. Even though clear differences could be observed, more realistic and distinct results would be achieved with a larger cross-sectional area (provided the surface area is consistent so that the load stays the same).

Fourth, the most realistic thermal results would have been made on live animal tissue. However, for the purpose of this experiment, tofu had the right properties to show clear thermal spread when exposed to electrosurgery, making is sufficient for the purpose of the measurements.

C. Future Research

The future research suggestions can be divided into two parts. First, the generation of more design requirements outside the technical and safety framework. Second, suggestions for the next steps for the design of the ESU.

Expansion of the design requirements:

Even though essential technical and safety design requirements have already been discussed in the report, four possible expansions of the requirements are suggested:

1) *AC Leakage:* An expansion of leakage tests are suggested. The "HF leakage" test conducted in the Property Tests was the measure of HF current to ground. An AC leakage test is also suggested, which is the measurement of low frequency current from the chassy and patient-connected probes to earth ground. The purpose is to prevent low frequency electric shock [9] to the operator, user or patient.

2) *Repairability:* An assessment of the internal hardware would give an insight to the repairability of current ESUs. Through this assessmentit can be seen how many parts can be aquired off the shelf and how much was produced by the company itself. Furthermore, through reverse engineering ideas can be gathered for an own ESU design.

3) *Usability:* By asking a surgeon to test and compare the three ESUs would give an insight to their usability. The user interface and performance can be assessed to set design requirements in that field too.

4) *Regulatory Requirements:* This includes governmental laws, industrial standards, and product regulations. These are important to consider in medical device designs, since bodies like the FDA approve the medical devices on the basis of the standards and regulations.

5) *Business Requirements:* This includes the cost analysis, schedule planning and other managemental requirements.

6) *LMICs Input:* Lastly, practitioners in LMICs should be asked what their design expectations would be for a new ESU design. Locals know the best where the

real limitations lie to make sure the product is a long lasting success.

Suggestions for the next design steps of a new ESU in a LMICs setting:

An extensive market assessment is suggested. A large number of ESUs exist, and there could be interesting partner companies that would help improve the access to electrosurgery worldwide.

The design of an ESU is a task which requires a multidisciplinary team. A suggestion would be to combine an industrial designer, electric engineer and biomedical engineer, where the tasks are split as following:
Industrial Designer:
- Packaging design,
- Interface design,
- Design of accessories.

Biomedical Engineer:
- Overview and management of the design & manufacturing,
- Development of software.

Electric Engineer:
- Design of electronic hardware.

To design an ESU for LMICs is challanging because limitations exist that developers in HICs underestimate or simply forget [4], [5]. According to Caldwell et al. [5] there are three approaches of HIC organizations to design or procure medical devices for LMICs. The most feasible design process should be assessed in order to ensure a qualitative high and long-term success.

1) *Appropriate Technology Approach ("We know what you need").* A device is designed due to the organizations perception of what is needed in a LMICs setting.
2) *Participatory Design Approach ("Tell us what you need, We'll design it").* The problem statement and evaluation of the final product is done together with the LMIC community. By asking the people at the local hospitals and medical centres their real requirements can be heard, leading to a more likely usage of the end product.
3) *Co-creation Approach ("Let's design together").* By going to the LMIC community and designing and fabricating the suggested device with the staff at hand. This design approach can largely increase the usage and effectiveness of the medical device, raise the probability that it will be maintained, and create the possibility that manufacturing could be made locally with available components.

D. Conclusion

In conclusion, a correlation between a low-end device being low-quality on all levels does not necessarily hold. The design requirements found through the Property Test and Thermal Camera Test form the first steps for a new and better ESU design. The most important ESU design requirements found for a LMICs setting include:
- An analogue and simple interface including a simple and dimensionless linearly increasing power control.
- The maximum power for cut should exceed 110 W and for coagulation 70 W.
- A clean sinusoid for the cut waveform and a clear duty cycle for the coagulation waveform ensure an effective thermal output.
- A control system preventing power drop with an increasing load improves surgical performance and reliability considerably.
- A light weight, a small size and a handle ensure transportability of the ESU. Universal spare parts and reusable equipment allow for repairability and an independence of the user to the manufacturer.
- HF leakage needs to be below 100 mA to prevent burns to the user, staff and patient.
- To round off the design criteria, a split return electrode should be used for safety.

By considering the above mentioned design requirements, implemented by a multidisciplinary team, a new generation of affordable high quality Electrosurgical devices can be developed. This would ensure better access to safe surgery in low to middle income countries.

REFERENCES

[1] "World Bank country and lending groups," https://datahelpdesk.worldbank.org/knowledgebase/articles/906519, accessed: 15.01.2018.

[2] J. G. Meara, A. J. Leather, L. Hagander, B. C. Alkire, N. Alonso, E. A. Ameh, S. W. Bickler, L. Conteh, A. J. Dare, J. Davies *et al.*, "Global surgery 2030: evidence and solutions for achieving health, welfare, and economic development," *The Lancet*, vol. 386, no. 9993, pp. 569–624, 2015.

[3] R. Malkin, *Medical instrumentation in the developing world.* Engineering World Health, 2006.

[4] K. Diaconu, Y.-F. Chen, C. Cummins, G. J. Moyao, S. Manaseki-Holland, and R. Lilford, "Methods for medical device and equipment procurement and prioritization within low-and middle-income countries: findings of a systematic literature review," *Globalization and health*, vol. 13, no. 1, p. 59, 2017.

[5] A. Caldwell, A. Young, J. Gomez-Marquez, and K. R. Olson, "Global health technology 2.0," *IEEE pulse*, vol. 2, no. 4, pp. 63–67, 2011.

[6] *Electrocut 100: Bistouri Electrique Manuel Utilisateur*, Recherche Dévelopement Electronique.

[7] A. Taheri, P. Mansoori, L. F. Sandoval, S. R. Feldman, D. Pearce, and P. M. Williford, "Electrosurgery: part i. basics and principles," *Journal of the American Academy of Dermatology*, vol. 70, no. 4, pp. 591–e1, 2014.

[8] C. W. Wallwiener, T. K. Rajab, B. Krämer, K. B. Isaacson, S. Brucker, and M. Wallwiener, "Quantifying Electrosurgery-Induced Thermal Effects and Damage to Human Tissue: An Exploratory Study with the Fallopian Tube as a Novel In-Vivo In-Situ Model," *Journal of Minimally Invasive Gynecology*, vol. 17, no. 1, pp. 70–77, 2010.

[9] M. G. Munro, "Fundamentals of electrosurgery part i: Principles of radiofrequency energy for surgery," in *The SAGES Manual on the Fundamental Use of Surgical Energy (FUSE)*. Springer, 2012, pp. 15–59.

[10] A. I. Brill, "Principles and practice of electrosurgery," *Reconstructive and Reproductive Surgery in Gynecology*, p. 18, 2010.

[11] A. L. Wallace, R. M. Hollinshead, and C. B. Frank, "The scientific basis of thermal capsular shrinkage," *Journal of shoulder and elbow surgery*, vol. 9, no. 4, pp. 354–360, 2000.

[12] P. J. Weber, B. R. Moody, R. M. Dryden, and J. A. Foster, "Electrosurgical standing cutaneous cone modification," *Dermatologic surgery*, vol. 27, no. 11, pp. 960–962, 2001.

[13] S. J. Hernandez-Divers, "Radiosurgery and laser in zoological practice: separating fact from fiction," *Journal of Exotic Pet Medicine*, vol. 17, no. 3, pp. 165–174, 2008.

[14] G. Bran, M. Moch, K. Hörmann, and B. Stuck, "Electrosurgical concepts in ent medicine. history, fundamentals and practice," *Hno*, vol. 55, no. 11, pp. 899–911, 2007.

[15] T. L. Smith and J. M. Smith, "Electrosurgery in otolaryngology– head and neck surgery: principles, advances, and complications," *The Laryngoscope*, vol. 111, no. 5, pp. 769–780, 2001.

[16] C. Hawthorne, "understanding radiofrequency," *Australian Cosmetic Surgery*, 2004.

[17] J. D. Nguyen, R. Crumley, and B. J.-F. Wong, "Overview of electrosurgery in head and neck surgery," in *Lasers in Surgery: Advanced Characterization, Therapeutics, and Systems XII*, vol. 4609. International Society for Optics and Photonics, 2002, pp. 260–266.

[18] G. A. Vilos and C. Rajakumar, "Electrosurgical generators and monopolar and bipolar electrosurgery," *Journal of minimally invasive gynecology*, vol. 20, no. 3, pp. 279–287, 2013.

[19] M. Schwartz, C.-J. Jeng, and L. T. Chuang, "Laparoscopic surgery for gynecologic cancer in low-and middle-income countries (lmics): An area of need," *Gynecologic oncology reports*, vol. 20, pp. 100–102, 2017.

[20] S. Gabriel, R. Lau, and C. Gabriel, "The dielectric properties of biological tissues: Iii. parametric models for the dielectric spectrum of tissues," *Physics in Medicine & Biology*, vol. 41, no. 11, p. 2271, 1996.

[21] R. L. Bussiere, "Guide to Performance and Safety Testing," 1998.

[22] H. A. Peterson, *Physeal injury other than fracture*. Springer Science & Business Media, 2012.

[23] C. J. Slager, J. Schuurbiers, J. Oomen, and N. Bom, "Electrical nerve and muscle stimulation by radio frequency surgery: role of direct current loops around the active electrode," *IEEE transactions on biomedical engineering*, vol. 40, no. 2, pp. 182–187, 1993.

[24] N. Van de Berg, J. Van den Dobbelsteen, F. Jansen, C. Grimbergen, and J. Dankelman, "Energetic soft-tissue treatment technologies: an overview of procedural fundamentals and safety factors," *Surgical endoscopy*, vol. 27, no. 9, pp. 3085–3099, 2013.

[25] F. M. B. Bisinotto, R. A. Dezena, L. B. Martins, M. C. Galvão, J. M. Sobrinho, and M. S. Calçado, "Burns related to electrosurgery–report of two cases," *Brazilian Journal of Anesthesiology (English Edition)*, vol. 67, no. 5, pp. 527–534, 2017.

[26] R. Gade and T. B. Moeslund, "Thermal cameras and applications: a survey," *Machine vision and applications*, vol. 25, no. 1, pp. 245–262, 2014.

[27] *Electrosurgical Generator: Force FX™Electrosurgical Generator*, Valleylab, 2012.

[28] G. C. Hulley, S. J. Hook, and P. Schneider, "Optimized split-window coefficients for deriving surface temperatures from inland water bodies," *Remote Sensing of Environment*, vol. 115, no. 12, pp. 3758–3769, 2011.

[29] P. Verboven, A. K. Datta, N. T. Anh, N. Scheerlinck, and B. M. Nicolai, "Computation of airflow effects on heat and mass transfer in a microwave oven," *Journal of Food Engineering*, vol. 59, no. 2-3, pp. 181–190, 2003.

[30] O. Al Sahaf, I. Vega-Carrascal, F. Cunningham, J. McGrath, and F. Bloomfield, "Chemical composition of smoke produced by high-frequency electrosurgery," *Irish journal of medical science*, vol. 176, no. 3, pp. 229–232, 2007.

[31] C. Guo, L. Zhou, and J. Lv, "Effects of expandable graphite and modified ammonium polyphosphate on the flame-retardant and mechanical properties of wood flour-polypropylene composites," *Polymers and Polymer Composites*, vol. 21, no. 7, pp. 449–456, 2013.

[32] S. Sarang, S. K. Sastry, and L. Knipe, "Electrical conductivity of fruits and meats during ohmic heating," *Journal of Food Engineering*, vol. 87, no. 3, pp. 351–356, 2008.

[33] S. Moizuddin, L. Johnson, and L. Wilson, "Rapid method for determining optimum coagulant concentration in tofu manufacture," *Journal of food science*, vol. 64, no. 4, pp. 684–687, 1999.

[34] T. Cai and K.-C. Chang, "Processing effect on soybean storage proteins and their relationship with tofu quality," *Journal of Agricultural and Food Chemistry*, vol. 47, no. 2, pp. 720–727, 1999.

[35] R. Dodde, A. Shih, and A. P. Advincula, "A Novel Technique for Demonstrating the Real-Time Subsurface Tissue Thermal Profile of Two Energized Surgical Instruments," *Journal of Minimally Invasive Gynecology*, vol. 16, no. 5, pp. 599–603, 2009. [Online]. Available: http://dx.doi.org/10.1016/j.jmig.2009.05.018

[36] T. L. de Jong, L. H. Pluymen, D. J. van Gerwen, G.-J. Kleinrensink, J. Dankelman, and J. J. van den Dobbelsteen, "Pva matches human liver in needle-tissue interaction," *Journal of the mechanical behavior of biomedical materials*, vol. 69, pp. 223–228, 2017.

SUMMARY OF APPENDICES

Appendix A: Selection Process of the Most Important Fields of Investigation for ESU Design Requirements

To design an Electrosurgical Unit (ESU) for LMICs, design requirements are needed. By comparing three existing ESUs a (1) technical, (2) safety, (3) repairability, and (4) usability tests could theoretically be made to reverse engineer design requirements. In order to focus the study, the four tests were evaluated on their usefulness in generating new design requirements. In conclusion a technical and safety analysis would give the best insight to the existing ESUs, while the repairability and usability studies were taken out of the scope of this study.

Appendix B: Settings Selection for Electrosurgical Devices

The most comparable settings at both cut and coagulation mode were selected between three different electrosurgical units. The waveform, current level and peak-to-peak voltage was analysed at each setting and the most comparable settings were selected to conduct further experiments. For the RDE Electrocut 100 the "coagulation Normal" and "cut Normal" settings were chosen. For the Valleylab Force FXc the "coagulation Fulgurate" and "cut Pure" were chosen. For the ERBE ICC 300 the "coagulation Forced" and "cut 1" were chosen.

Appendix C: Property Test Pilot Study

Pilot test of the Property Test was made to determine the right parameters and test conditions.
First, the QA_ES II FLUKE Analyzer measurement error of the recorded data was determined through repeatability and through fast successive tests. Errors are compared to the errors given by the Manual. Second, the power values of the dimensionless power knob of the RDE are determined. Third, a minimum delay time between activating the ESU and measuring with the Analyzer was determined, to minimize the start-up error. Four, the increase sequence for the load in the tests was determined.

Appendix D: Property Test Protocol

A short version of the protocol used to conduct the property tests is included, allowing for a possible repetition of experiments by a third party.

Appendix E: Thermal Camera Test, Tofu Selection Process

To test if tofu is sufficient, three short cascading experiments—where the latter two are designed due to the open conclusions of the first—show the selection process of tofu. First, resistance of tofu is unsuccessfully attempted to be measured in Ohm. Second, an alternative to tofu is unsuccessfully searched for. Third, It is successfully investigated that the length of tofu influences its resistance. Furthermore, a pilot test is made of the Thermal Camera Test to determine the right tofu length and activation times used for the tests.

Appendix F: Thermal Camera Test Protocol

A short version of the protocol used to conduct the Thermal Camera Test is included, allowing for a possible repetition of experiments by a third party.

Appendix G: Thermal Camera Test Extended Result in Graphs, Figures and Tables

Additional graphs and figures are shown here, resulting from the Thermal Camera Test. First, graphs depicting over time the maximum temperatures and thermal damage. Second, image showing all tofu samples from after the experiments were conducted.

APPENDIX A
SELECTION PROCESS OF MOST IMPORTANT FIELD OF
INVESTIGATION FOR ESU DESIGN REQUIREMENTS

Abstract—**To design an Electrosurgical Unit (ESU) for LMICs, design requirements are needed. By comparing three existing ESUs a (1) technical, (2) safety, (3) repairability, and (4) usability tests could theoretically be made to reverse engineer design requirements. In order to focus the study, the four tests were evaluated on their usefulness in generating new design requirements. In conclusion a technical and safety analysis would give the best insight to the existing ESUs, while the repairability and usability studies were taken out of the scope of this study.**

Introduction

To design a new ESU that fits into a LMICs setting, critical design requirements are necessary. For this, different properties of three electrosurgical units (ESUs) are determined, namely *RDE Electrocut 100* (RDE), *Valleylab Force FXc* (Valleylab), and *ERBE ICC 300* (ERBE) (See Figure B.1) at monopolar settings. ESUs support the surgeon during his operations by cutting and coagulating tissue.

The design requirements determine what is needed to allow for the future design or—if more feasible—the purchase of an ESU. An ESU made for LMICs would have properties that are:

- robust,
- transportable,
- effective,
- affordable
- safe,
- repairable,
- equipped with sterilisable accessories,
- have a simple usability, and
- a low maintenance.

An selection of the most important of these properties needs to be made in order to gain the best information possible from the three ESUs.

Methods

The properties have been categorised into four subgroup tests. (1) a technical analyses of the properties, which includes investigating the physical properties of current devices such as robustness, transportability, effectiveness, cost and functional reliability; (2) safety for user, staff and patient; (3) repairability and maintenance; and (4) usability for the surgeon.

For this chapter, a selection process chart was used to test the four subgroups and they were ranked according to their usefulness in finding general design requirements. This includes the effectiveness of the tests to distinguish between the three ESUs, their ability to fulfil safety standards, help reduce costs, and that can show a level of quality and safety.

Results

The test subgroups and their usefulness standards to find general design requirements are summarised and evaluated in Table A.1. It was found that the technical and safety tests had a $+5$ effectiveness factor, repairability a -1 effectiveness factor and usability a 0 effectiveness factor.

Discussion & Conclusion

It was decided to lay the focus of this study only on the first two areas of investigation—namely the technical and safety aspects of the ESUs. Therefore repairability, maintenance and usability are out of the scope of this study.

TABLE A.1: Table showing selection process of most critical design requirements

		Important aspects to know for a new ESU Design for a LMIC Setting					
		Distinguishes ESUs	Shows fulfilled standards	Findings could help lower costs	Indicates quality	Shows safety	**TOTAL**
Tests	Technical	+ +	+	+	+ +	-	**5**
	Safety	+	+ +	-	+	+ +	**5**
	Repairability	+	- -	+	+	- -	**-1**
	Usability	+ +	-	-	+	-	**0**

APPENDIX B
SETTINGS SELECTION FOR ELECTRSURGICAL DEVICES

A. Settings Selection Process Report

Abstract—The most comparable settings at both cut and coagulation mode were selected between three different electrosurgical units. The waveform, current level and peak-to-peak voltage was analysed at each setting and the most comparable settings were selected to conduct further experiments. For the RDE Electrocut 100 the "coagulation Normal" and "cut Normal" settings were chosen. For the Valleylab Force FXc the "coagulation Fulgurate" and "cut Pure" were chosen. For the ERBE ICC 300 the "coagulation Forced" and "cut 1" were chosen.

Introduction

Different properties for three electrosurgical units (ESUs) are determined, namely *RDE Electrocut 100* (RDE), *Valleylab Force FXc* (Valleylab), and *ERBE ICC 300* (ERBE) (see Figure B.1) at monopolar settings. ESUs support the surgeon during his operations through the coagulation mode (stopping of bleeding) and the cut mode (cutting of tissue) [9]. The three ESUs have a large set of settings. Comparable settings are selected for both cut and coagulation modes to effectively draw conclusions between the three devices.

All experiments involving the RDE will use the "Normal Coagulation" and "Normal Cut" settings. The only "Epilation coagulation/cut" alternative setting is meant for hair removal [6], which is not considered part of the projects scope [6]. Therefore the setting selection of the ERBE and Valleylab (See Table B.1) are based on the "Normal Coagulation/Cut" settings of the RDE and the requirement that the cut setting has a continuous waveform and the coagulation waveform has a duty cycle.

TABLE B.1: Setting options for ERBE ICC 300 and Valleylab Force FXc

ERBE		Valleylab	
Coagulation	Cut	Coagulation	Cut
Soft	1	Desiccate	Low
Forced	2	Fulgurate	Pure
Spray	3	Spray	Blend
–	4	–	–

Methods

Using the *QA_ES II FLUKE Electrosurgical Analyzer* (Analyzer) measuring device the wave shape and peak-to-peak Voltage (V_{pp}) were measured for each of the ERBE and Valleylab settings. First the wave shape was compared and the cut settings with a duty cycle or the coagulation settings with a continuous waveform were discarded. Following this selection, the V_{pp} was compared to the RDE measurements, also obtained with the Analyzer. The setting most similar to the RDE "Normal" mode was then chosen for further experiments.

Results

The results for the coagulation mode settings are shown in Figure B.2. The "Valleylab Fulgurate" and "ERBE Forced" settings are the most comparable to the "RDE Normal setting".

The results for the cut mode settings are shown in Figure B.3. The "Valleylab Pure" setting is the most comparable to the "RDE Normal setting". For ERBE all four cut mode settings were very similar. After some further measurements, it was found that the cut settings only change in bipolar surgery. Therefore, for simplicity, the devices default setting "1" was chosen for all experiments.

TABLE B.2: Coagulation mode settings of Valleylab Force FXc and ERBE ICC 300 compared to RDE Electrocut 100 at $P = 35\,\text{W}$, $L = 200\,\Omega$

Coagulation Setting	Wave Form	Current	V_{PP}
RDE Normal	*Duty Cycle*	*410 mA*	*550 V*
Valleylab Desiccate	Continuous	–	–
Valleylab Fulgurate*	Duty Cycle	399 mA	669 V
Valleylab Spray	Duty Cycle	390 mA	706 V
ERBE Soft	Continuous	–	–
ERBE Forced*	Duty Cycle	390 mA	787 V
ERBE Spray	Duty Cycle	377 mA	832 V

* Setting most comparable to RDE Electrocut 100

TABLE B.3: Cut mode settings of Valleylab Force FXc and ERBE ICC 300 compared to RDE Electrocut 100 at $P = 55\,\text{W}$, $L = 200\,\Omega$

Cut Setting	Wave Form	Current	V_{PP}
RDE Normal	*Continuous*	*533 mA*	*571 V*
Valleylab Low	Continuous	503 mA	310 V
Valleylab Pure*	Continuous	502 mA	307 V
Valleylab Blend	Duty Cycle	–	–
ERBE 1*	Continuous	522 mA	333 V
ERBE 2	Continuous	523 mA	327 V
ERBE 3	Continuous	523 mA	327 V
ERBE 4	Continuous	523 mA	326 V

* Setting most comparable to RDE Electrocut 100

Discussion & Conclusion

For ERBE-Coagulation the "Forced" sub-setting was chosen, while for ERBE-Cut setting "1" was chosen. For Valleylab-Coagulation the "Fulgurate" setting was chosen, while Valleylab-Cut setting "Pure" was chosen. The exact impact of the different settings could have been explored in more detail, however, the tests made already show high comparability.
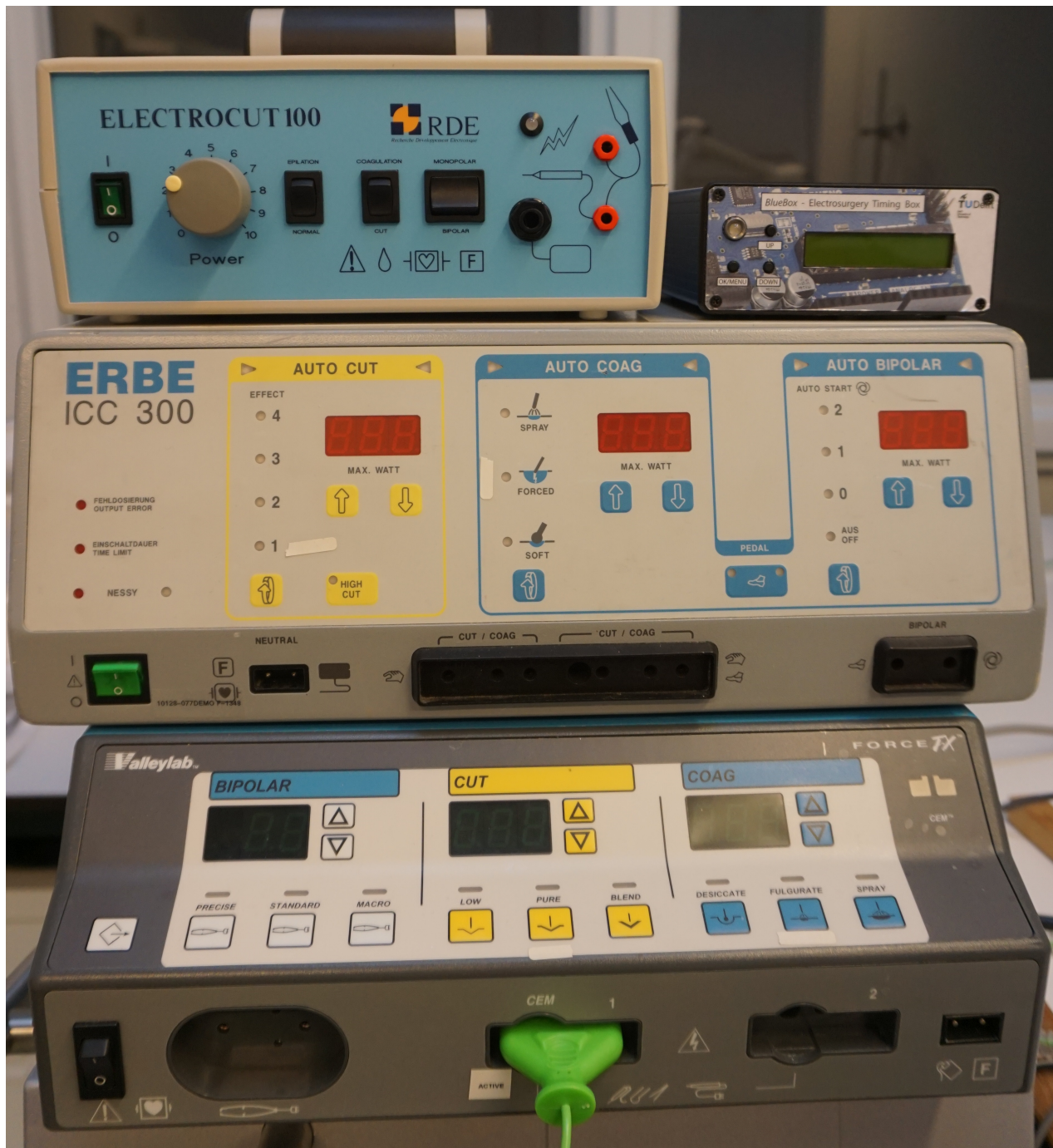
B. Apparatus

Fig. B.1: Figure showing all three ESUs and a timebox. *Top left:* RDE Electrocut 100, *Top right:* Time box, *Middle:* ERBE ICC 300, *Bottom:* Valleylab Force FXc

APPENDIX C
PROPERTY TEST PILOT STUDY

Abstract—**As part of determining the differences between three different electrosurgical devices, a property test will be made using the *QA_ES II FLUKE Electrosurgical Analyzer*. To be able to design the protocol for the experiments, various pilot studies had to be made in order to understand the electrosurgical units as well as measuring device.**

Experiment 1: The electrosurgical device *RDE Electrocut 100* has dimensionless power knob with a scale between 0–10. What these power values mean in wattage needs to be found. For each setting (0–10) the real power was measured. It was found that the power follows a $\log(x)$ trajectory with a maximum power of $P_{coag} = 70\,\mathrm{W}$ and $P_{cut} = 110\,\mathrm{W}$.

Experiment 2: As a part of determining properties of different electrosurgical devices, a repeatability test of the measuring device was made. At different set power and modes, the current, real power and V_{pp} were measured eight times with a time of $10\,\mathrm{s}$ in between. It was found that the measuring device reliably measures data repeatedly.

Experiment 3: As a part of determining properties of different electrosurgical devices, an optimal delay time needs to be found between the activation of the electrosurgical device and the measurement itself. Delay times between 200–$1000\,\mathrm{ms}$ were measured against current, peak-to-peak voltage and Power. The most optimal time delay found was $500\,\mathrm{ms}$.

Experiment 4: For the property measurement of different electrosurgical devices, the load range of interest needs to be found to obtain an informative and sufficient sequence resolution. Three different load sequences were tested against current, power and V_{pp}. The best sequence was a linear high resolution sequence at low loads and an exponential increase in load values at loads higher than $150\,\Omega$.

A. Power Test for RDE Electrocut 100

Abstract—**The electrosurgical device *RDE Electrocut 100* has dimensionless power knob with a scale between 0–10. What these power values mean in wattage needs to be found. For each setting (0–10) the real power was measured. It was found that the power follows a $\log(x)$ trajectory with a maximum power of $P_{coag} = 70\,W$ and $P_{cut} = 110\,W$.**

Introduction

The *RDE Electrocut 100* (RDE) is an electrosurgical device used mainly in Low-Middle Income Countries (LMICs). Both the coagulation mode (stopping of bleeding) and the cut mode (cutting of tissue) can be selected on the device to support the surgeon during his operations.

As a measure of intensity the surgeon operating the device can change the power settings on a dimensionless knob between a scale of 0-10. The exact wattage of the scale needs to be found in order to be able to conduct further property tests on the RDE.

Methods

The *QA_ES II FLUKE Electrosurgical Analyzer* is used to measure the power of the RDE over its dimensionless scale between 1-10 (at a rated load of $200\,\Omega$). At every scale unit, the real power was measures in Watt for both the coagulation and cut modes. All tests were repeated twice.

Results

The results can be seen in Figure C.1. The maximum power at the setting 10 is $110\,W$ for cut mode and $70\,W$ for coagulation mode.
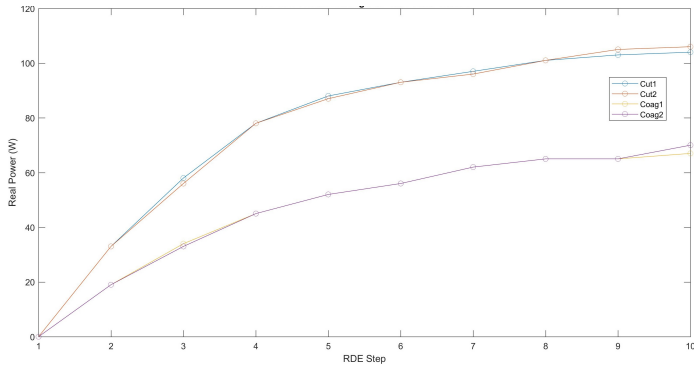
Fig. C.1: Real power vs set power of the RDE Electrocut 100.

Discussion & Conclusion

The increase in power is non-linear, approximately following an approximate $\log(x)$ trajectory. How effective this trajectory is needs to still be determined. Compared to the Valleylab Force FXc and ERBE ICC 300 (both coagulation:$P_{max} = 110\,W$ cut: $P_{max} = 110\,W$), the maximum powers achieved for the RDE were low.

B. Consecutive time test for QA_ES FLUKE Electrosurgical Analyzer

Abstract—**As a part of determining properties of different electrosurgical devices, a repeatability test of the measuring device was made. At different set power and modes, the current, real power and V_{PP} were measured eight times with a time of $10\,s$ in between. It was found that the measuring device reliably measures data repeatedly.**

Introduction

The *QA_ES II FLUKE Electrosurgical Analyzer* (Analyzer) was used to determine different properties for the *RDE Electrocut 100* (RDE), *Valleylab Force FXc* (Valleylab), and ERBE ICC 300 (ERBE). These three electrosurgical units (ESUs) support the surgeon during his operations through the coagulation mode (stopping of bleeding) and the cut mode (cutting of tissue).

As a reliability test, the stability in rapid testing repeatability needs to be determined.

Methods

For all three ESUs eight tests were made with 10 seconds in between. The coagulation mode was tested at a power of $33\,W$, $90\,W$, and $110\,W$. The cut mode was tested at a power of $20\,W$, $50\,W$, and $70\,W$. For every test the power, V_{pp}, and current were tested over time and all results were compared.
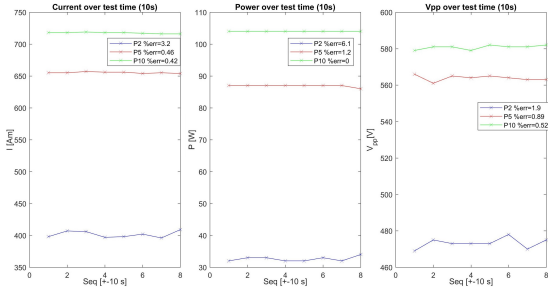
Results

The results of the RDE, ERBE and Valleylab can be seen in Figures C.2, C.3, and C.4 respectively. There were slight errors in the data for high powers (<5%). At the setting of $33\,W$ the error was up to 6.5%.
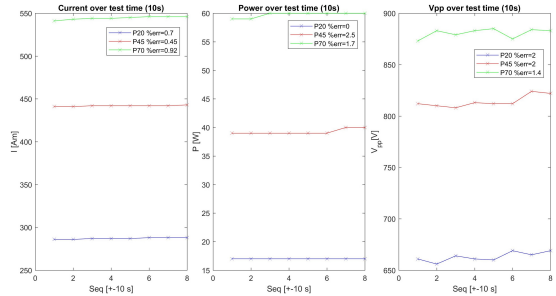
Discussion & Conclusion

For all three ESUs there was no recognizable change or pattern in data over the rapid test repetitions. This shows that the Analyzer can be used many times consecutively without the risk that the data will distort over time.
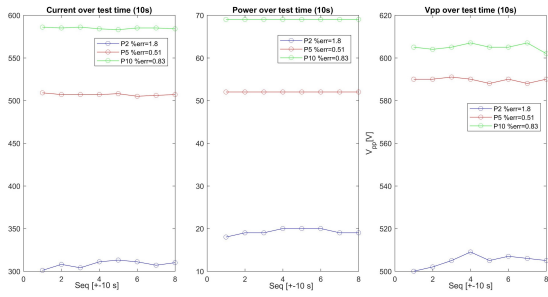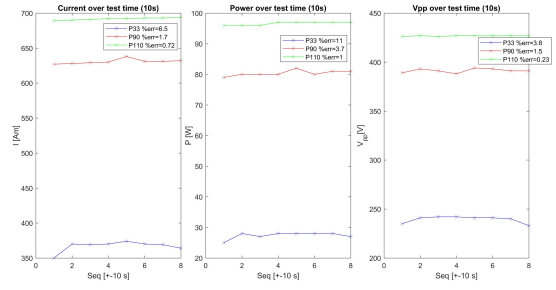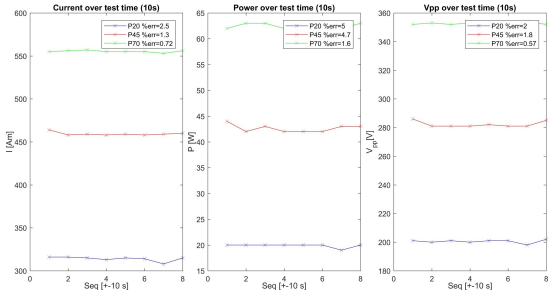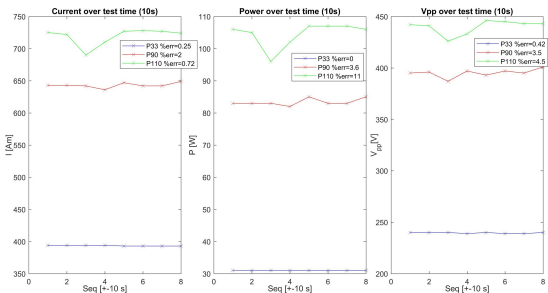
(a) RDE Coagulation mode

(b) RDE cut mode

Fig. C.2: Time test for Analyzer using the *RDE Electrocut 100*. Every 10 seconds the *QA_ES II FLUKE Electrosurgical Analyzer* was activated to test if the results changed with many consecutive tests. It can be seen that there is no patterned change in data over time.

(a) ERBE Coagulation mode

(b) ERBE Cut mode

Fig. C.3: Time test for Analyzer using the E*ERBE ICC 300*. Every 10 seconds the *QA_ES II FLUKE Electrosurgical Analyzer* was activated to test if the results changed with many consecutive tests. It can be seen that there is no patterned change in data over time.

(a) Valleylab coagulation mode

(b) Valleylab cut mode

Fig. C.4: Time test for Analyzer using the *Valleylab Force FXc*. Every 10 seconds the *QA_ES II FLUKE Electrosurgical Analyzer* was activated to test if the results changed with many consecutive tests. It can be seen that there is no patterned change in data over time.

C. Delay test for QA_ES FLUKE Electrosurgical Analyzer

Abstract—**As a part of determining properties of different electrosurgical devices, an optimal delay time needs to be found between the activation of the electrosurgical device and the measurement itself. Delay times between 200–1000 ms were measured against current, peak-to-peak voltage and Power. The most optimal time delay found was 500 ms.**

Introduction

The *QA_ES II FLUKE Electrosurgical Analyzer* (Analyzer) is used to determine different properties for the *RDE Electrocut 100* (RDE), *Valleylab Force FXc* (Valleylab), and ERBE ICC 300 (ERBE). These three electrosurgical units (ESUs) support the surgeon during his operations through the coagulation mode (stopping of bleeding) and the cut mode (cutting of tissue).

As a setting option for the Analyzer, a delay can be selected. In other words, the Analyzer first starts the ESU, and after a delay the measurement is only started. This ensures that the measurement is not made before the ESU has started up properly. However, how much delay is needed for the three ESUs to start up properly is not known.

Methods

The Analyzer can be set to a delay of 200–1000 ms in steps of 100 ms. The RDE was tested twice at [200, 400, 600, 1000] ms delay. The ERBE and Valleylab were tested once only at [200, 400, 600] ms. The coagulation mode was tested at a power of 33 W, 90 W, and 110 W. The cut mode was tested at a power of 20 W, 50 W, and 70 W. For every test the current, V_{pp}, and power were tested over delay time and all results were compared.

Results

The results of the RDE, ERBE and Valleylab can be seen in Figures C.5, C.7, and C.6 respectively. For all three ESUs the delay time did not make a difference in the current, V_{pp}, and power measurements, except for the Valleylab-coagulation mode (See Figure C.6). At the Valleylab-coagulation mode, the current and power measurements were lower that measurements with a higher delay time.

Discussion & Conclusion

Since Valleylab coagulation mode struggled to reproduce values at low delay times, the extra high value of 500 ms was chosen, having a safety factor over 2.
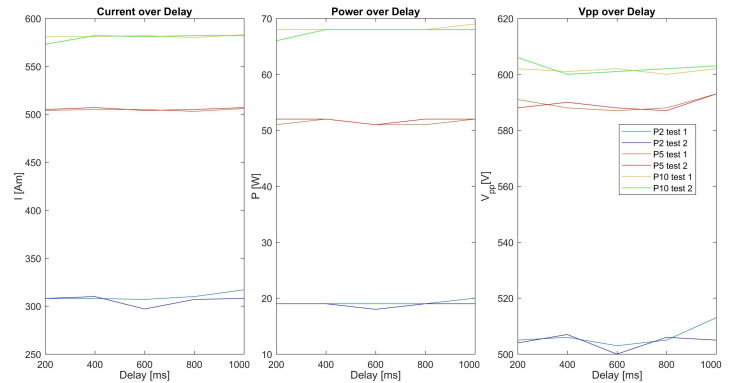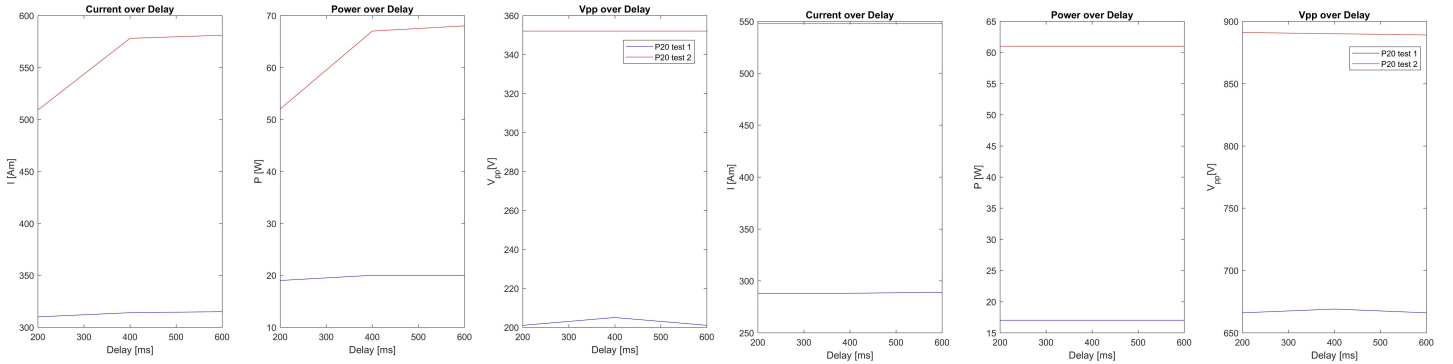

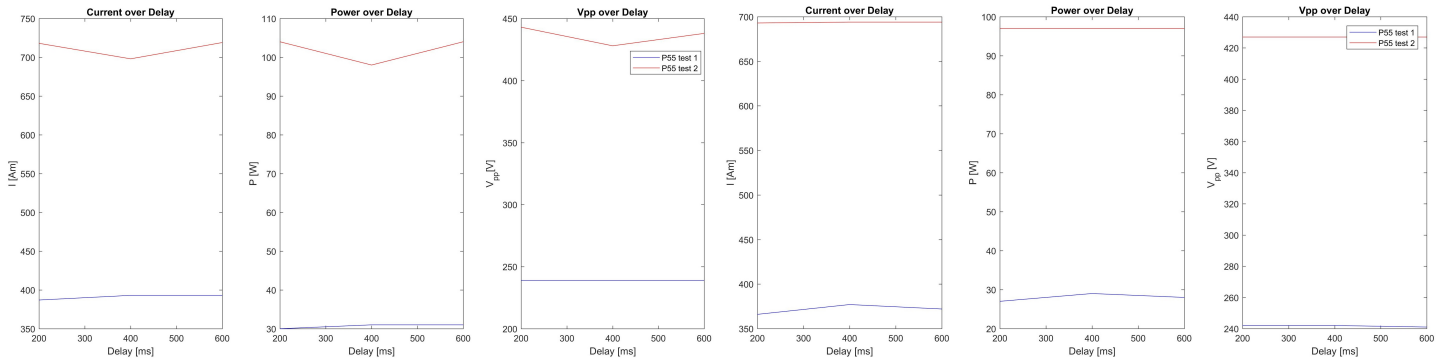
(a) RDE coagulation mode
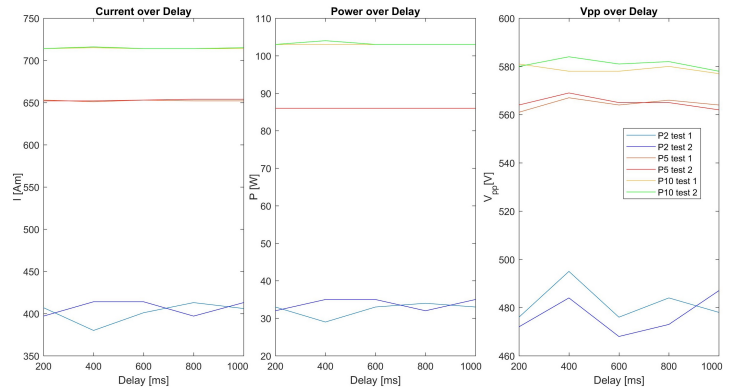
(b) RDE cut mode

Fig. C.5: RDE Electrocut behaviour of delay time between activating the ESU and taking the current, power or V_{pp} measurements. (a) indicates the coagulation mode delay behaviour. (b) indicates the cut mode delay behaviour.

(a) Valleylab coagulation mode

(a) ERBE coagulation mode

(b) Valleylab cut mode

(b) ERBE cut mode

Fig. C.6: Valleylab Force FXc behaviour of delay time between activating the ESU and taking the current, power or V_{pp} measurements. (a) indicates the coagulation mode delay behaviour. (b) indicates the cut mode delay behaviour.

Fig. C.7: ERBE ICC 300 behaviour of delay time between activating the ESU and taking the current, power or V_{pp} measurements. (a) indicates the coagulation mode delay behaviour. (b) indicates the cut mode delay behaviour.

D. Load Test Sequence spacing

Abstract—**For the property measurement of different electro-surgical devices, the load range of interest needs to be found to obtain an informative and sufficient sequence resolution. Three different load sequences were tested against current, power and V_{pp}. The best sequence was a linear high resolution sequence at low loads and an exponential increase in load values at loads higher than $150\,\Omega$.**

Introduction

The *QA_ES II FLUKE Electrosurgical Analyzer* (Analyzer) is used to determine different properties for the *RDE Electrocut 100* (RDE), *Valleylab Force FXc* (Valleylab), and ERBE ICC 300 (ERBE). These three electrosurgical units (ESUs) support the surgeon during his operations through the coagulation mode (stopping of bleeding) and the cut mode (cutting of tissue).

As part of the property test the power drop over an increasing tissue load is tested. The Analyzer allows for load settings of 10–$2500\,\Omega$ in steps of $25\,\Omega$ and 2500–$5200\,\Omega$ in steps of $100\,\Omega$. Since these are a lot of load settings, a selection of the load sequence needs to be made to make tests that are as informative as possible, without taking too much time.

Methods

As a restriction, a load sequence of less than 13 loads were suggested. It was assumed that low loads need to have a better resolution than large loads, since they double faster (e.g $25*2 = 50$, while $3000*2 = 6000$). In Figure C.8 the three sequences selected can be seen. First, a *linear sequence* was chosen, where each value was $500\,\Omega$ apart. Second, an *exponential sequence* was chosen, where the following equation $X_{n+1} = X_n * 2$ was used with $X_n = 25\,\Omega$. Third, a combination between linear and exponential was chosen, dubbed the *resultant sequence*. Between 25–$150\,\Omega$ linear steps of $25\,\Omega$ were made. From $150\,\Omega$ onwards the values were exponentially increasing by $X_n = (X_n - X_{n-1}) * 2 + X_{n-1}$.

All three sequences were tested on the RDE at maximum power for coagulation and cut modes.

Results

In Figures C.9a and C.9b the results can be seen for the coagulation and cut modes respectively. For the current measurements the *resulting sequence* showed the highest peak current at around $200\,\Omega$ and little difference between the sequences in readings at larger loads.

In the power measurement, which is the most important measurement to consider, the *linear* and *exponential sequences* showed noise at high loads. The *resulting sequence* showed a good resolution at low loads and a smooth curve at higher loads.

For the V_{pp} measurement, a high resolution at low loads was not necessary. In general the *linear sequence* showed large amounts of fluctuations, while the *resulting sequence* showed necessary detail at low loads.

Discussion & Conclusion

At low loads, a high resolution is needed, since is was here where the magnitudes of the current, power and V_{pp} changed the most. The *linear sequence* and *exponential sequence* did not show enough information at mainly low loads. With the *resulting sequence*, the best and most reliable information could be extracted from the data and should be considered for the further property experiments regarding electrosurgical devices.
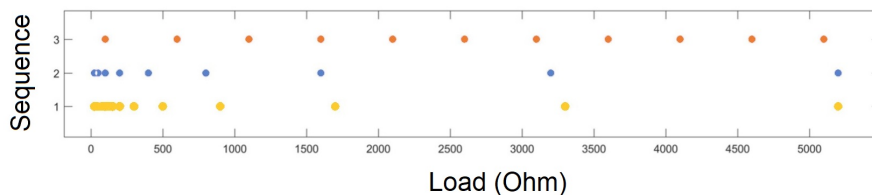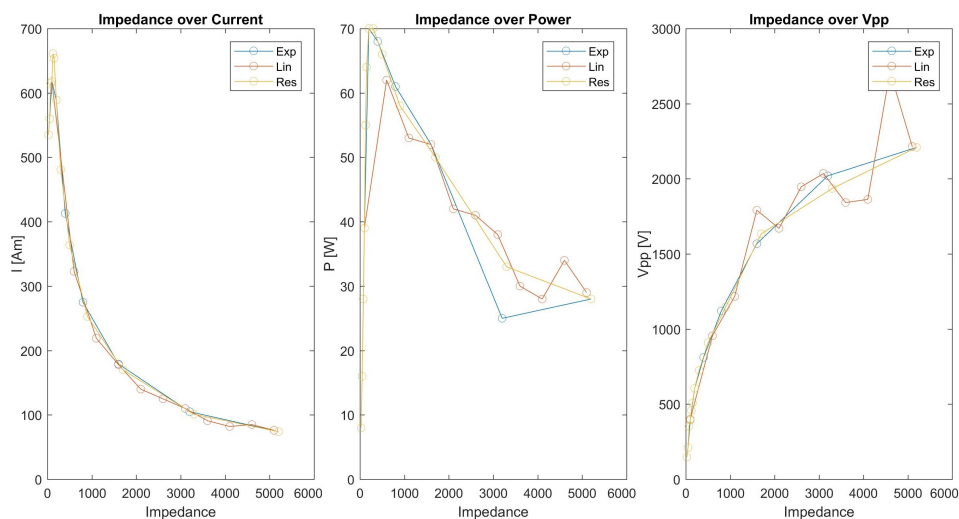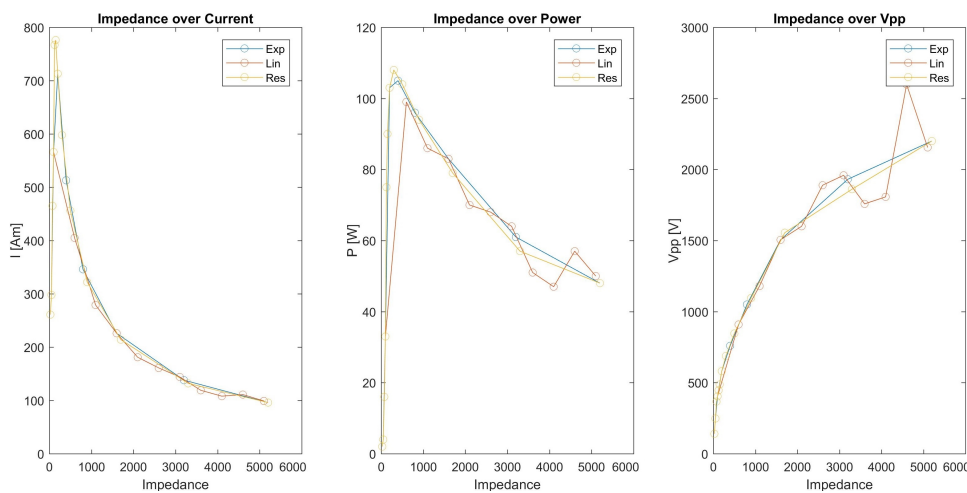
Fig. C.8: Different measuring sequences are tested to see where the most detailed resolution is needed. Three following three sequences are suggested: Linear, Exponential, Resultant.

(a) RDE coagulation mode at $P = 70\,\mathrm{W}$

(b) RDE cut mode at $P = 110\,\mathrm{W}$

Fig. C.9: Sequences tested on electrocal current (*left*), real power (*middle*) and V_{pp} (*right*) with the RDE. It can be seen that at low loads, a high resolution is required.

APPENDIX D
PROPERTY TEST PROTOCOL

Introduction[8]

This experiment aims to investigate and compare the properties of different Electrosurgical Unit (ESU). In the experiments, it will be only looked at monopolar cases. Power Output Tests and Radio Frequency (RF) Leakage tests will be made. The Power Output Tests measure peak-to-peak voltage (V_{pp}), current (I), crest factor (CF) and power (P). The RF leakage measures how much current leaks out of the device, causing potential damage to the equipment or people.

Research questions:

1) Does each device differ from the properties they claim to have in the manual?
2) How do the results compare between the ESUs?

    a) Set Power vs Real Power
    b) Waveform shapes in Cut and Coagulation modes
    c) Power drop: Real Power vs Leakage.

3) How does the safety between the devices compare?

    a) Leakage test
    b) Return electrode safety measures

4) Is the use of this test valuable to determine the quality of an ESU?

The leakage test is done to prevent thermal damage to unintended patient tissue. Capacitive coupling can be, in part, responsible for serious patient complications. Some methods used to minimize capacitive coupling are active electrode shielding, dispersive metal cannulas, sheathed guide wires, and bipolar active electrodes.

Methods

The QA_ES II FLUKE Analyzer is used to measure the property of each ESU. The tests will be conducted according

[8]A more detailed version of the Thermal Camera Test Protocol with all the raw results tables can be found digitally on request by the author.

to the manual. See in Appendix, section QA_ES II, for an introduction to the device, where all the functionalities used in this document are described. For each of the three ESUs the test procedures will be the same.

Material List

General Material needed for all tests:
- QA_ES II FLUKE Analyzer
- Computer with Picoscope 6 software
- Paper
- Pen

RDE Electrocut 100 Property test:
- RDE Electrocut 100
- 4x 4mm banana plug to banana plug cables
- 1x $\frac{1}{4}$ inch phone connector to banana socket cable
- RDE foot switch simulator:
  - 1x DIN 3 connectors to DB9 female.
  - 1x DB9 male to 5 x 4mm banana sockets indicating cut, coag & bipolar footswitch/common.
- 1x 25cm x21cm metal plate connected to ground.
- 1x Picoscope measuring meter with USB adaptor.

RDE Electrocut 100 leakage test:
- RDE Electrocut 100
- RDE Electrocut 100 foot switch with DIN 3 connector
- 4x 4mm banana plug to banana plug cables
- 1x $\frac{1}{4}$ inch phone connector to banana socket cable
- 1x power/earth: socket to plug IEC power cable with earth connector via 4mm banana socket
- 1x 25cm x21cm metal plate connected to ground.

Valleylab Force FX-c Property test:
- Valleylab Force FX-c
- 3x 4mm banana plug to banana plug cables
- Force FX-c footswitch simulator:
  - 1x Amphenol 3-pin and 4-pin connectors to DB9 female.
  - 1x DB9 male to 5 x 4mm banana sockets indicating cut, coag & bipolar footswitch/common.
- 1x Resistor: 47 Ohm resistor between a 4mm banana plug pin and socked (Enable activation)
- 1x Picoscope measuring meter with USB adaptor.

Valleylab Force FX-c leakage test:
- Valleylab Force FX-c
- Valleylab Force FX-c footswitch with Amphenol 3-pin and 4-pin connectors.
- 3x 4mm banana plug to banana plug cables
- 1x power/earth: socket to plug IEC power cable with earth connector via 4mm banana socket
- 1x Ground plate cable with 2x 4mm banana pin outlets
- 1x Resistor: 47 Ohm resistor between a 4mm banana plug pin and socked (Enable activation)

Erbe ICC 300 Property test:
- Erbe ICC 300
- 3x 4mm banana plug to banana plug cables
- 1x Erbe footswitch simulator:
  - 1x Binder 4-pin connector to DB9 female.
  - 1x DB9 male to 5 x 4mm banana sockets indicating cut, coag & bipolar footswitch/common.
- 1x Picoscope measuring meter with USB adaptor.

Erbe ICC 300 leakage test:
- Erbe ICC 300
- Erbe ICC 300 foot switch with binder 4-pin connector
- 3x 4mm banana plug to banana plug cables
- 1x power/earth: socket to plug IEC power cable with earth connector via 4mm banana socket
- 1x Erbe footswitch: Binder 4-pin connector to 4mm banana sockets
- 1x Ground plate cable with 2x 4mm banana pin outlets

Steps to follow

Before start of the experiment:
1) Ensure that the set-up is correct.
2) It is ensured that both the Analyzer and the ESU are on.
3) Computer is connected with the Oscilloscope and the PicoScope Software is started.
4) A picture of the setup is taken.

During the experiment:
1) After every new test ensure that the cables are connected correctly.
2) Ensure that the settings on the Analyzer are correct.

For each experimental condition:
1) Connect the device correctly and set the conditions on the Analyzer
2) Start measurement
3) Save frequency shape on the oscillometer.
4) Once the Analyzer finished the measurement, write down voltage (V_{PP}), Current (*I*), Crest factor (*CF*) and Power (*P*).

Power Output Test

In the Single Operation mode, the Analyzer makes a single measurement of the ESU output after the set delay time. When the measurement is complete, the test automatically stops. Make connections between the Analyzer and the ESU as shown in Figure D.2.

To run a test in Single Operation Mode:
1) Press **F2** until an asterisk (*) symbol appears following 'Mode'.
2) Rotate the encoder knob until the ***Singl. Oper** test mode appears on the screen, and then press the **Enter** key.
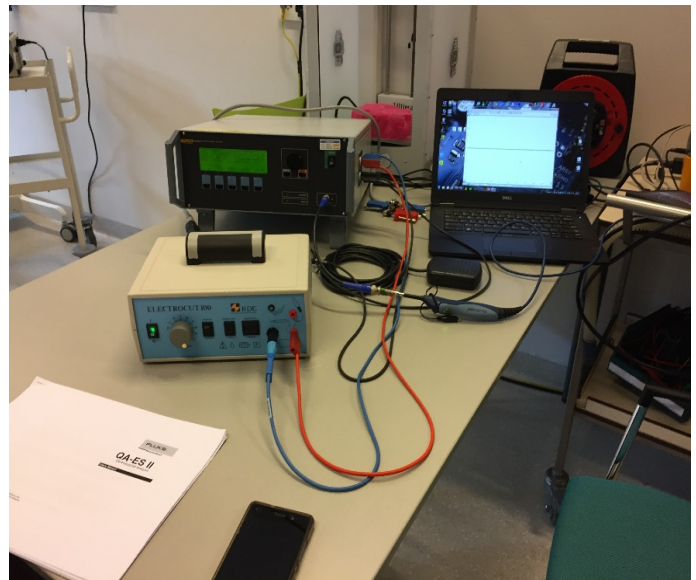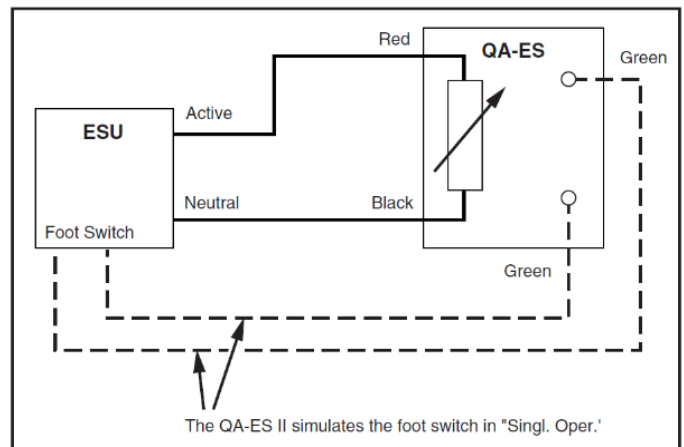

Fig. D.1: Figure: Image of the experimental set-up.

Fig. D.2: Figure: Power Output Test connection set-up.

3) Set the test **Load** as required for the test.
4) Set the **Delay** time as required for the test.
5) Set and activate the ESU.
6) Press **START (F3)** to take a measurement. After the set delay, the Analyzer records the values and displays them on the screen. Copy these results to a table.

RF Leakage test

There are four test setups to accomplish this leakage testing according to the QA_ES II manual, however, others say that the last test is not needed, since it measures the current flowing back into the ESU, instead of measuring the leakage [21]. Hence only the three tests are made. The ESU must operate at the maximum output setting in each operating.

To run an HF Leakage Test, perform the following steps:

1) Connect the Analyzer to the ESU to test leakage from the Active electrode using the appropriate setup, as shown under " HF Isolated Equipment" or " Ground HF Equipment."
2) Press **F2** until an asterisk (*) symbol appears following 'Mode'.
3) Rotate the encoder knob until the ***RF Leakage** test mode appears on the screen, and then press the **Enter** key.
4) Set the ESU as prescribed by the manufacturer for leakage tests and then activate the ESU.
5) With the ESU activated, press **START (F3)**; the Analyzer takes the leakage measurement. Copy these results to a table.
6) Repeat steps for all circuit set-ups shown in FiguresD.3 and D.4.

The limits for the acceptable leakage currents depend upon the test configuration. The Manual of the Analyzer indicates the limits as shown in Table 1. These values are possibly derived from the California Medical Instrumentation Association, where leakage needs to be less than 150 mA or less than 4.5 W to earth ground at 200 Ohm. The standards of IEC 60601-2-2 says this:

BEGIN QUOTE ["
19.3.101 Thermal effects of HF LEAKAGE CURRENTS

In order to prevent unintended thermal burns, HF LEAKAGE CURRENTS tested from ACTIVE and NEUTRAL ELECTRODES with PATIENT CIRCUITS activated shall, depending on their design, comply with the following requirements.

1) HIGH FREQUENCY LEAKAGE CURRENTS

   a) NEUTRAL ELECTRODE referenced to earth The PATIENT CIRCUIT is isolated from earth but the NEUTRAL ELECTRODE is referenced to earth at HIGH FREQUENCIES by components (for example a capacitor) satisfying the requirements of a TYPE BF APPLIED PART. When tested as described below, the HF LEAKAGE CURRENT flowing from the NEUTRAL ELECTRODE through a non-inductive 200 ? resistor to earth shall not exceed 150 mA.
   b) NEUTRAL ELECTRODE isolated from earth at HIGH FREQUENCY The PATIENT CIRCUIT is isolated from earth at both high and low frequencies, and the isolation shall be such that the HF LEAKAGE CURRENT flowing from each electrode through a $200\,\Omega$ non-inductive resistor to earth does not exceed 150 mA when tested as described below.
   Compliance is checked by the following test. The HF SURGICAL EQUIPMENT is set up as described for test 1 of 19.3.101 a) 1), the output being unloaded and loaded at the

RATED LOAD. Any metal ENCLOSURES of CLASS II HF SURGICAL EQUIPMENT and INTERNALLY POWERED HF SURGICAL EQUIPMENT shall be connected to earth. HF SURGICAL EQUIPMENT having an insulating ENCLOSURE shall be positioned on earthed metal having an area at least equal to that of the base of the HF SURGICAL EQUIPMENT, during this test. The HF LEAKAGE CURRENT is measured from each electrode in turn while the HF SURGICAL EQUIPMENT is operated at maximum output setting in each HF SURGICAL MODE.

"] END QUOTE

The value of 150 mA is to prevent interference with other medical equipment in a theatre and to prevent the patient to be accidentally exposed to hazardous coupling to ground. I could not find out yet how exactly they came up with the value of 150 mA.

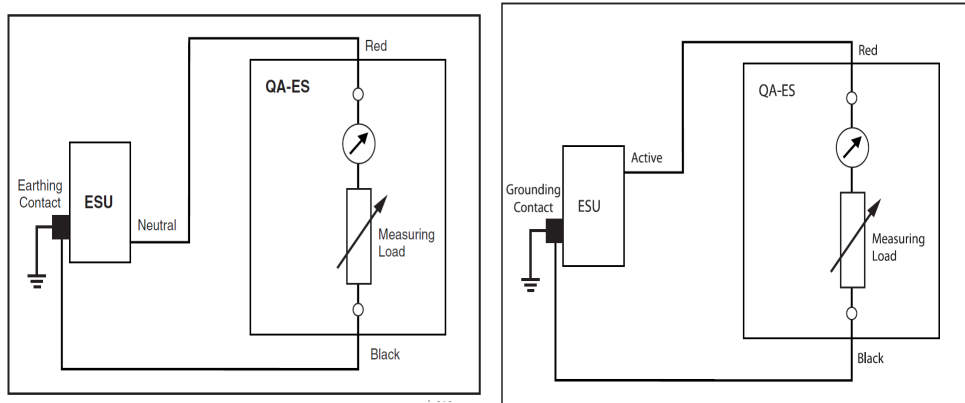| Test Configuration	Limits of Acceptable Leakage Current
Measured on electrodes	The leakage current should not exceed 150 mA.
Bipolar	The leakage current should not exceed 1 % of the maximum bipolar rated power output.
Measured at equipment terminals	The leakage current should not exceed 100 mA.

Fig. D.3: Figure: Not loaded RF-leakage test set-up
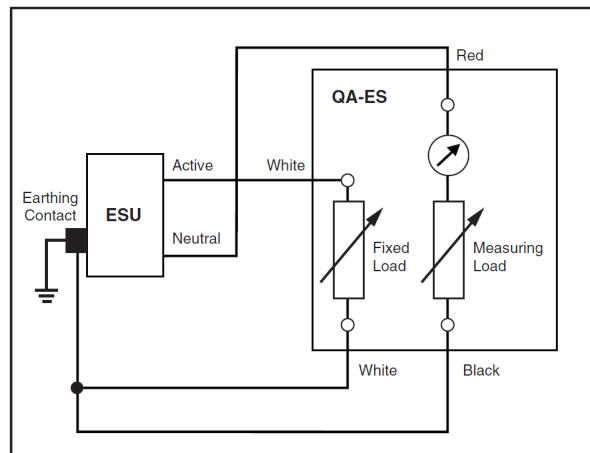

Fig. D.4: Figure: Loaded RF-leakage test set-up

Experimental Conditions

The Experiments are randomized with MATLAB 2017 function randperm(). Randomization checks if the results change with a device that heats up over time.

Power Output Test—Coagulation

TEST 1: Property over Power

Set-up	Power Output Test Set-up
Device	**RDE, valleylab, ERBE**
State	Coagulation
Power	*0–Max in 10 steps*
Device	**Analyzer**
Mode	Single Operation Test
Load	200 Ohm
Delay	500 ms

TEST 2: Power over Load

Set-up	Power Output Test Set-up
Device	**RDE, Valleylab, ERBE**
State	Coagulation
Power	40W, Max
Device	**Analyzer**
Mode	Single Operation Test
Load	*25–5600 Ohm*
Delay	500 ms

Power Output Test—Cut

TEST 3: Property over Power

Set-up	Power Output Test Set-up
Device	**RDE, Valleylab, ERBE**
State	Cut
Power	*0–Max in 10 steps*
Device	**Analyzer**
Mode	Single Operation Test
Load	200 Ohm
Delay	500 ms

TEST 4: Power over Load

Set-up	Power Output Test Set-up
Device	**RDE, Valleylab, ERBE**
State	Cut
Power	40W, Max
Device	**Analyzer**
Mode	Single Operation Test
Load	*25- 5600 Ohm*
Delay	500 ms

RF Leakage Tests—Coagulation

Set-up	RF leakage Test
Device	**RDE, Valleylab, ERBE**
State	Coagulation
Power	Max
Device	**Analyzer**
Mode	RF Leakage
Load	200 Ohm
Delay	500 ms

RF Leakage Tests—Cut

Set-up	RF leakage Test
Device	**RDE, Valleylab, ERBE**
State	Cut
Power	Max
Device	**Analyzer**
Mode	RF Leakage
Load	200 Ohm
Delay	500 ms

APPENDIX E
THERMAL CAMERA TEST TOFU SELECTION PROCESS

Summary—**Electrosurgical units (ESU) are used as an essential operating tool to assist the surgeon on various operations. By heating target tissue through high frequency (HF) electrical current, many types of tissues can be cut and coagulated using a metallic instrument or needle [7]. Once activated, the current runs from the active to the neutral electrode through the body, where the body acts as a resistive load. An alternative material representing this resistive load of the body needs to be found that has similar properties and that is non-animalistic (vegan) [9]. In the Thermal Camera Test (TCT) (see Appendix F) the temperature spread is tested on the new material.**
Tofu has been suggested by Roos Oosting (MISIT Laboratory Phd candidate), since it is organic and tissue-like. To test if tofu is sufficient, three short cascading experiments—where the latter two are designed due to the open conclusions of the first—show the selection process of tofu.
Experiment 1: **Resistance of tofu is measured. FLUKE 117 Multimeter is used on *JUMBO Veggie Chef Naturel Tofu*. Extremely high resistance was measured. Tofu changes its resistance considerably at magnitude of current, frequency of current, temperature of the tofu, water content of tofu and the coagulant used. In conclusion, either a different measure of tofu resistance needs to be found, or an alternative material.**
Experiment 2: **An alternative material in comparison to tofu is looked for. PVC is compared to tofu and MatWeb is used to find a new material similar to organic tissue. PVC melts and degenerated as soon as it is exposed to electrosurgery. MatWeb was unable to find a suitable alternative to tofu. In conclusion, an alternative way needs to be found to control resistance of tofu.**
Experiment 3: **As an alternative measure to a multimeter for tofu resistance, it is hypothesized that tofus resistive load measure (L) behaves according to $L = \frac{l}{A\sigma}$. Using different lengths of tofu (l) at the same cross sectional area (A) the burn intensity of the RDE Electrocut 100 is measured by eye at maximum cut and coagulation settings. In conclusion, the length of tofu can be used as a consistent measure for resistance in tofu. Using $l < 2\,\mathrm{cm}$ for low resistance measure and $l >= 2\,\mathrm{cm}$ for a high resistance measure is sufficient.**

---

[9]MISIT laboratorium (TU Delft) does not allow for scientific testing on animal tissue.

(a) FLUKE 117 Multimeter was used to measure the resistance of tofu

(b) *JUMBO Veggie Chef Naturel Tofu* used in experiments
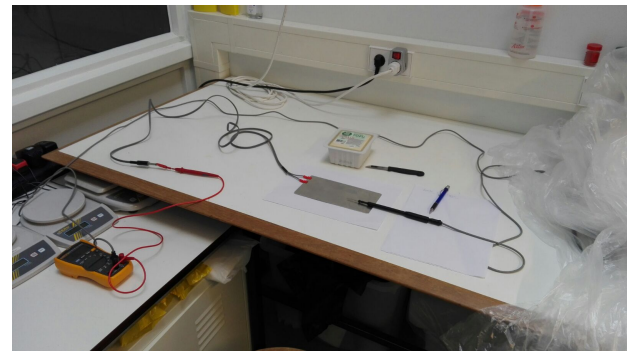
Fig. E.1: Experimental equipment used.

Fig. E.2: Experiment 1: experimental set-up

A. Experiment 1: Tofu Resistance Measurement

Abstract—**In this experiment the resistance of tofu is measured by using the FLUKE 117 Multimeter on *JUMBO Veggie Chef Naturel Tofu*. Extremely high resistance could be measured. Tofu changed its resistance considerably at magnitude of current, frequency of current, temperature of the tofu, water content of tofu and coagulant used. In conclusion, an alternative measure of tofu resistance or an alternative material need to be found.**

Introduction:
Following the property test (Appendix F), the power drop with a higher resistance was investigated thermally through a thermal camera on tofu samples. A set resistive load and a clear thermal spread on the sample is needed to be found. Furthermore, the sample material should be organic to have a tissue-like behaviour to HF currents.
To see what the different power/load settings do thermally, a thermal test was designed. For this, the resistance of tofu needs to be known.

Methods:
For testing the resistance of TOFU the FLUKE 117 Multimeter (Figure E.1a) and samples of *JUMBO Veggie Chef Naturel Tofu* (Figure E.1b) at [1, 2]cm x 7cm x 4cm were used (i.e. tofu between electrodes are [1, 2]cm). The tofu was placed on the RDE Electrocut 100 ground plate(experimental set-up in Figure E.2). The neutral and active electrodes were connected to the multimeter and the active electrode touched the one side of the tofu. The measurement is then read and recorded. Furthermore, the resistivity was measured by putting two plates on either side of the tofu to increase the current density at the points of contact.

Results:
A resistance of between $1 - 3\,\mathrm{M\Omega}$ was measured. The resistivity measured resulted in similar results.

Discussion & Conclusion:
The experiment is regarded as failed. This result of the resistance did not adhere to the expected values between $0 - 5\,\mathrm{k\Omega}$. Furthermore, no set resistance was found for tofu.
It is assumed that the reason for the high resistance is that with a larger frequency, magnitude current and temperature the resistance drops considerably and therefore a experiment designed like this will fail. On the same samples the RDE Electrocut 100 was tested at the highest power setting,

showing visible activation. That means, according to the property tests power drop, the resistance of tofu at that point should be below $5\,\mathrm{k\Omega}$.

In papers it shows that resistance goes down with higher frequency [20] and human tissue has a resistance of $100\,\Omega \cdot \mathrm{cm}$(Brain(gray))–$200\,\Omega \cdot \mathrm{cm}$(muscle, cartilage)–$1070\,\Omega \cdot \mathrm{cm}$(Bone) [20]. We assume Tofu to be somewhere in between.

There are alternatives for using the thermal camera test set-up. Either an alternative measure of tofu resistance or an alternative material need to be found:

1) The first option is to use a material, like a silicone, that handles heat to above $250°C$ and that will not change its impedance with an increasing current, frequency and temperature considerably. This will not be an organic or flesh type material, but it will give a reliable comparison between the three devices. What this material would be and where to find it is unknown yet, however, fire retardant materials might have the wanted property.
2) Secondly, the conductivity of $\sigma = \frac{LI}{AV} = \frac{L}{AR}$ is known. In this equation L is the length and A the cross-sectional area of the sample, R is the internal resistance of the sample, I is current and V is voltage. This formula shows that the resistance of the material is linearly proportional to its length [32]. If we take three set samples of tofu with three different lengths (e.g. $[1]cm \cdot [1]cm \cdot [1, 2, 3]cm$), it is known that there are three linearly different resistances. However, the resistance and the thickness L to be used would be unkown; it is only known that the resistance is low enough for current to flow. In conclusion, it could be compared how the ESUs handle a changing resistance.
3) Thirdly, the piece of tofu is kept at a constant size where only the change in power is measured. It is true, that due to the changing magnitude and frequency of the current–and the different subsequent temperatures– will cause the the resistance of the tofu to be different. Therefore, the data would not fit exactly on the property test. However, it could be seen how the ESUs are able to perform under different power conditions.

Fig. E.3: Experimental set-up to test if PVA or tofu is a better material to replace animal tissue in a electrsurgical thermal test.
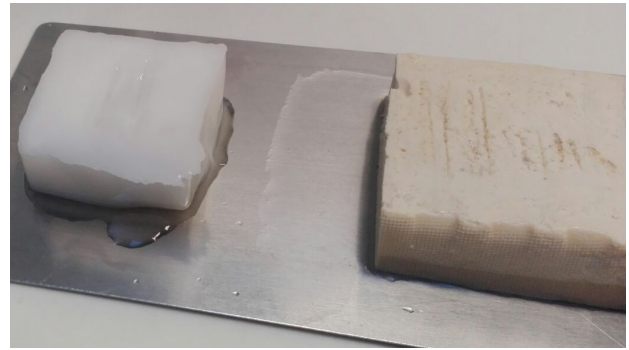

Fig. E.4: On the left it can be seen that the PVA dissolves with electroheating it and on the right tofu can be seen, which physically behaves more like tissue.

B. Experiment 2: Alternative Material to Tofu for TCT

Abstract—**Experiment 2: In this experiment it is looked for an alternative material in comparison to tofu. PVC is compared to tofu and MatWeb is used to find a new material similar to organic tissue. PVC melted and degenerated as soon as it is exposed to electrosurgery. MatWeb was unable to find a suitable alternative to tofu. In conclusion, an alternative way to control resistance of tofu needs to be found.**

Introduction:
As a first option it is proposed to use tofu as the resistance component for the circuit, however, this is not a steady material to use. Tofu, just as most organic materials [32], changes its resistivity depending on the type (there are over 13) [34] and amount [33] of coagulant in the tofu. When considering that the water content also changes between samples, a consistent tofu resistance is hard to find. Why do we not use tofu, which uses a single coagulant, from the same producer? The problem with organic material is that its resistance changes considerably depending on the (1) magnitude of the current, the (2) frequency of the current and the (3) temperature of the biological material [32]. In the thermal camera test, the current level, frequency and temperature distribution is wanted to be changed, causing the resistance to consequently vary significantly too.
Consequently, without knowing the tofu resistance at the test conditions, tofu will not provide a reliable and consistent material to observe the effect of waveforms depending on the resistance and power settings nor will it show the relationship between power and load drop reliably. Therefore, an alternative is searched for.
The new material should have a similar electrical resistivity, Young's Modulus, and thermal resistivity/melting point than biological tissue.

Methods:
PVA is a possible material that could simulate tissue in thermal experiments because it has similar mechanical properties [36]. The PVA is exposed to cut and coagulation modes and compared to tofu at the same settings. The experimental set-up can be seen in Figure E.3.

On MatWeb a material is searched for with the following properties:
1) $300 - 1000°C$
2) Electrical resistivity of $25 - 1000\,\Omega$cm
3) Young's Modulus of Elasticity 0.0005-0.9 GPa

Results:
Regarding the PVA test it can be concluded that this material does not resist heat well and that it melts away very quickly (See Figure E.4). Therefore, it is not suitable to test the different electro surgical devices.

The search on MatWeb resulted in 21 suggested materials shown in Figure E.5. However, the materials were vague with plastics having a high range of properties, making them unusable.

Discussion & Conclusion:
No alternative material was found that could replace animal tissue. An alternative way to measure of resistance needs to be found for the existing tofu samples.

Choose up to 3 Material Properties
Set the range by entering the minimum and/or maximum values for each selected property.

| Melt Temperature (20562 matls) | ▼ |

Min: 300   Max: 1000   Unit: °C ▼

Submit the Query (**Required**)
Click on the 'Find' button below to submit the query.

| Electrical Resistivity (28545 matls) | ▼ |

Min: 25   Max: 1000   Unit: ohm-cm ▼

FIND   RESET

| Modulus of Elasticity (40655 matls) | ▼ |

Min: 0.0005   Max: 0.9   Unit: GPa ▼

Found 21 Results -- Page 1 ▼ of 1 -- [Prev Page] [Next Page] -- view 50 ▼ per page

Select		Material Name	Melt Temperature (°C)	Electrical Resistivity (ohm-cm)	Modulus of Elasticity (GPa)
☐	1	Overview of materials for Aluminum Alloy	593 - 816	0.00000260 - 1.20e+16	0.0480 - 342
☐	2	Overview of materials for Polycarbonate/ABS Alloy, Unreinforced	199 - 330	100 - 1.00e+18	0.00240 - 10.3
☐	3	Overview of materials for Nylon 6, Unreinforced	200 - 330	10.0 - 1.00e+17	0.350 - 13.0
☐	4	Overview of materials for Nylon 6, Impact Grade	210 - 330	100 - 1.00e+16	0.145 - 15.0
☐	5	Overview of materials for Nylon 6, Heat Stabilized	138 - 304	1.00 - 1.00e+16	0.470 - 20.0
☐	6	Overview of materials for Nylon 6, 20% Glass Fiber Filled	193 - 370	1000 - 1.00e+17	0.0630 - 14.3
☐	7	Overview of materials for Nylon 66, Impact Grade	220 - 310	1.00 - 1.00e+16	0.600 - 41.4
☐	8	Overview of materials for Nylon 66, 30% Glass Fiber Filled	230 - 340	1000 - 1.00e+18	0.220 - 15.0
☐	9	Overview of materials for Nylon 610	215 - 310	5.00 - 1.00e+16	0.450 - 44.2
☐	10	Overview of materials for Polycarbonate, Impact Modified	220 - 338	10.0 - 1.00e+17	0.225 - 3.95
☐	11	Overview of materials for Polyetherimide (PEI)	232 - 427	0.100 - 1.00e+18	0.0370 - 42.0
☐	12	Overview of materials for Polyimide	399 - 416	0.100 - 4.00e+19	0.107 - 46.9
☐	13	Overview of materials for Polyphthalamide (PPA)	240 - 360	0.200 - 1.00e+17	0.500 - 48.3
☐	14	Overview of materials for Polypropylene, Molded	160 - 320	1000 - 1.00e+18	0.00800 - 8.25
☐	15	Overview of materials for Polypropylene, Extrusion Grade	160 - 330	1000 - 1.00e+18	0.680 - 3.60
☐	16	Overview of materials for Polypropylene, Flame Retardant	160 - 302	10.0 - 1.00e+17	0.800 - 9.31
☐	17	Overview of materials for Polypropylene Copolymer	145 - 302	50.0 - 1.00e+17	0.100 - 6.20
☐	18	Overview of materials for Polyphenylsulfone (PPSU)	321 - 399	10.0 - 1.00e+17	0.0689 - 8.14
☐	19	Overview of materials for PVC, Flexible Grade	110 - 310	2.50 - 5.60e+15	0.00552 - 0.0121
☐	20	Overview of materials for PVC, Wire and Cable Grade	110 - 310	2.50 - 5.60e+15	0.00600 - 1.12
☐	21	RTP Company RTP 3199 X 117877 B Perfluoroalkoxy (PFA), Carbon Nanotube - Electrically Conductive - High Purity	343 - 385	100	0.689

Fig. E.5: Materials suggested by MatWeb suitable to show reliable thermal images with a steady load gave umbiguous results. The ranges selected were a minimum melting point 300°C, electrical resistivity of 25–1000Ω and a modulus of elasticity below 0.9 GPa

C. Experiment 3: Alternative Resistance Measure for Tofu

Abstract—**Experiment 3: As an alternative measure to a multimeter for tofu resistance, it is hypothesized that tofus resistive load measure (L) behaves according to $L = \frac{l}{A\sigma}$. Using different lengths of tofu (l) at the same cross sectional area (A) the burn intensity of the RDE Electrocut 100 is measured by eye at maximum the cut and coagulation settings. In conclusion, the length of tofu can be used as a consistent measure for resistance in tofu. Using $l < 2\,\text{cm}$ for low resistance measure and $l >= 2\,\text{cm}$ for a high resistance measure is sufficient.**

Introduction:
Tofu changes its resistance considerably at magnitude of current, frequency of current, temperature of the tofu, water content of tofu and the coagulant used. If, for each case, all variables are kept constant, the tests can be compared. An alternative unit to the standard resistance Ohm(Ω) measure is needed.

It is hypothesized that tofu resistive load measure (L) behaves according to $L = \frac{l}{A\sigma}$, where l is the thickness tofu between the electrodes, A is the cross-sectional area and σ the electrical conductivity. A change in l would linearly increase or decrease the load. This can be used to have repeatable and comparable loads within the experiments.

Methods:
To test different resistances, different tofu thicknesses were taken to see what the effect between the samples was. Using different lengths of tofu (l) at the same cross sectional area (A), the burn intensity of the RDE Electrocut 100 was measured by eye at maximum cut and coagulation settings (see Figure E.6).

The burn intensity was measured according to high, medium and low burn intensity. Four different tofu lengths were used ($l = [0.5123]cm$) and tested with two power settings of $40W$ and maximum power (Cut: $70W$; Coagulation: $110W$).

Results:
At tofu lengths $l >= 2$ the burn intensity was medium at high and low power and $40W$. At tofu lengths $l <= 2$ the burn intensity was high at high and low power and $40W$.

Discussion & Conclusion:
There is a considerable difference in performance between thin and thick tofu thickness. This shows that a power drop can be recorded at different tofu lengths. In general using $l < 2\,\text{cm}$ as a low resistance and $l >= 2\,\text{cm}$ as a high resistance is sufficient for significantly different results in the Thermal Camera Test.

(a) Test set-up

(b) Close up of test set-up

Fig. E.6: Experiment 3

Appendix F
Thermal Camera Test Protocol

Introduction[10]

Research questions:

1) How do the 3 ESUs compare by:
   a) What were the maximum temperatures reached?
   b) What was the mean maximum temperature over the activation?
   c) What was the volume of the thermal tissue damage > 60 degrees?
   d) What was the volume of the thermal tissue damage > 100 degrees?

2) Questions that can be answered:
   a) How much did each ESU react to a changing power setting?
   b) How much did each ESU react to a changing load?
   c) How much did each ESU react to a changing waveform setting?
   d) How well did the devices produce expected values from literature?

Method

The FLIR A35 Series Thermal Camera will be used to measure the temperature changes. The images are saved as .mat files and analysed using MATLAB. Experimental Set-up can be found in Figure 6.

Material List:
- FLIR A35 Series Thermal Imaging Camera,
- Computer,
- Tofu test sample,
- ESU,
- Camera,
- Knife,

---

[10]A more detailed version of the Thermal Camera Test Protocol with all the raw results tables can be found digitally on request by the author.

- Ruler,
- 2 laboratory rigs for holding the camera and active electrode of the ESU.

Steps to follow

Before start of the experiment:
1) A double check that the set-up is correct will be made.
2) It is ensured that the power of the ESU and camera are on.
3) Distance between camera and active electrode of the ESU will be measured.
4) A picture of the setup will be taken.

During the experiment:
1) The distance between camera and active electrode should be kept similar
2) The position of the tofu sample can be changed, the active electrode should be kept on the same place
3) A photo is made of each samples after the experiment to evaluate the burn mark

Methods for Experimental Tests:
1) level horizontal surface into the wanted sizes (1 cm x 1 cm x 1cm; 1 cm x 1cm x 3 cm).
2) The tip of the active electrode is placed in the middle of the tofu sample.
3) The thermal camera is placed in 4 cm distance to the electrode tip
4) The smoke extractor is started at a setting of 45
5) The camera recording is started
6) The electrode is activated for 2 seconds
7) Six seconds later the camera is stopped
8) Video is saved as a .seq file.

Methods for the Data Analysis:
1) Convert files into .mat files using ThermaCAM Researcher Pro 2.10
2) Using Convert2SingleMATfile.m, convert all images to a single .mat file per video
3) Average the values of each cases three trials to make one video.
4) Find the maximum temperature per video
5) Find the mean maximum temperature over the activation in each case
6) Find the area of tissue over 60 deg and 100 deg.
7) Draw a table with results.

Experimental Conditions

The order of the experiments is randomized by using the randperm() function in MATLAB 2017b

TABLE F.1: Table showing Experimental conditions

Variable	Description	Variable No.	Experimental condition		
Time	Length of activation	1	2 seconds		
Wavelength	Wave shape and length	2	Cut	Coagulate	
Power	P=VI	2	40/110	40/70	
Trails	Number of experimental repEtions	3	n/a		
ESUs	Different ESU models	3	RDE	ERBE	Valleylab
Electrode tip	Changing current density	1	2 mm blade		
Load	Needs to be measured	2	1cm/3cm Tofu		
Total		*72*			

APPENDIX G
THERMAL CAMERA TEST EXTENDED RESULTS IN
GRAPHS, FIGURES AND TABLES

Summary—**Supplementary Figures for the Thermal Camera Test. Appendix G-A shows the thermal damage and maximum temperature measured over the activation and cooling periods of each tofu experiment. Appendix G-B shows the burn marks on the tofu samples of each tofu experiment.**

A. Maximum temperature and area over time
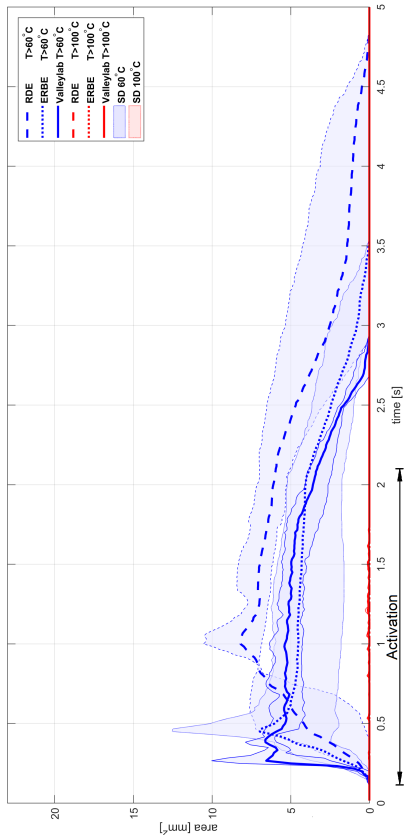
(a) Area over 50°C and 100°C at every time point.
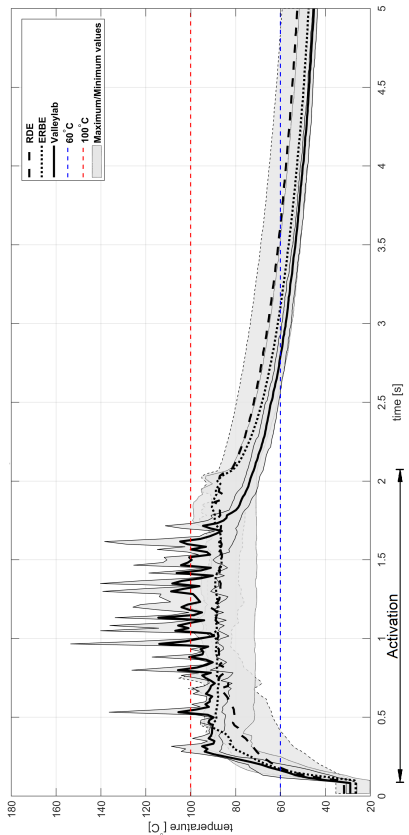
(b) Maximum Temperature over time.

Fig. G.1: Cut; Tofu=1 cm; P=40 W
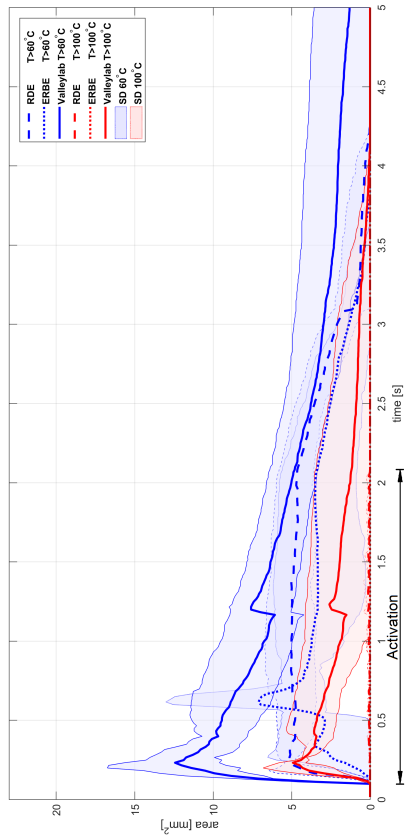
(a) Area over 50°C and 100°C at every time point.
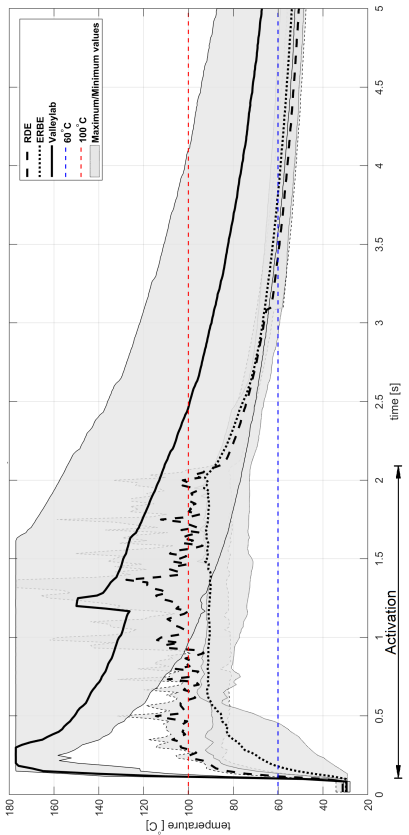
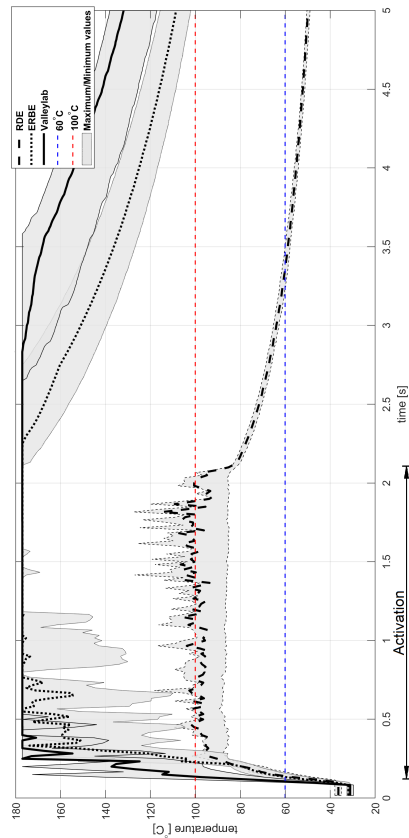(b) Maximum Temperature over time.

Fig. G.2: Cut; Tofu=1 cm; P=110 W
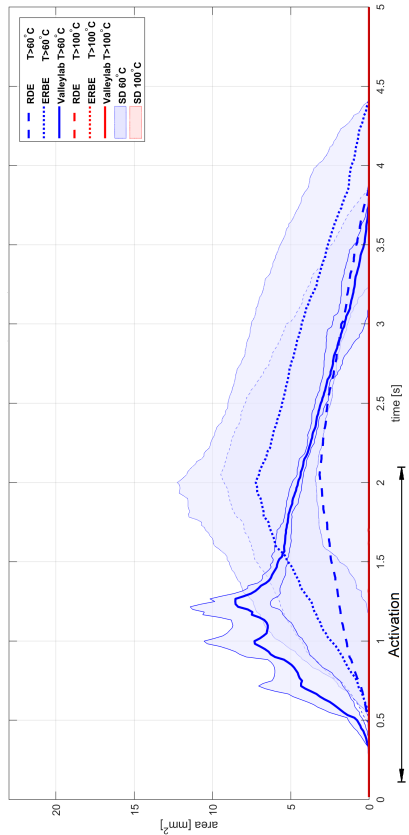
(a) Area over 50°C and 100°C at every time point.
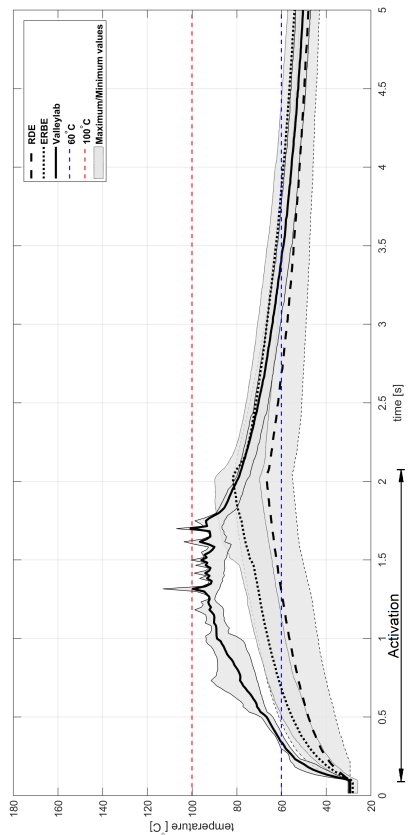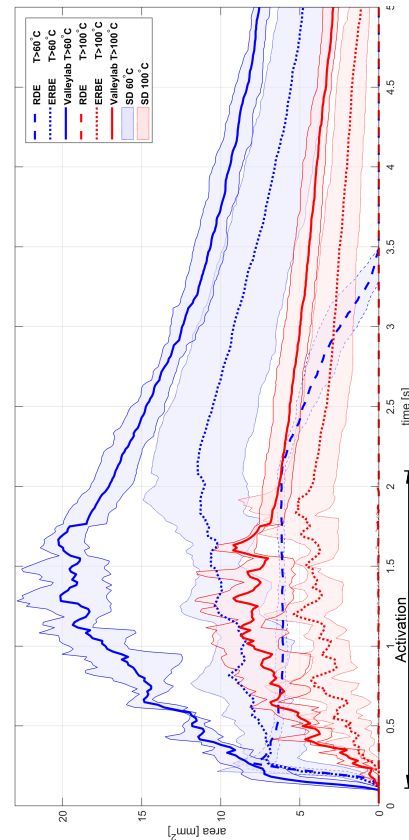
(b) Maximum Temperature over time.

Fig. G.3: Cut; Tofu=3 cm; P=40 W
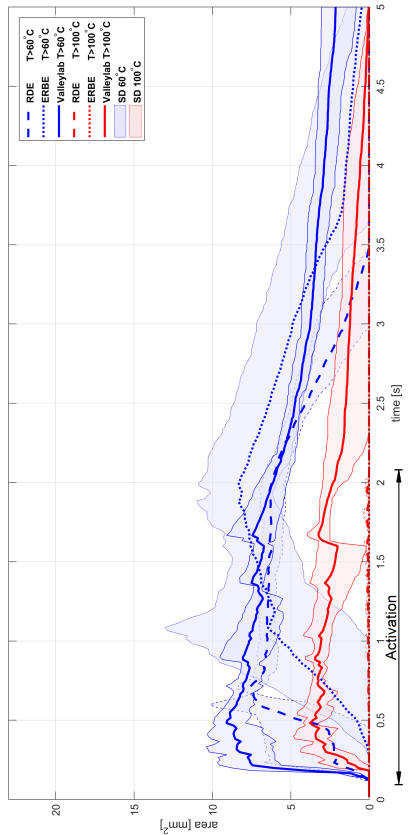
(a) Area over 50°C and 100°C at every time point.
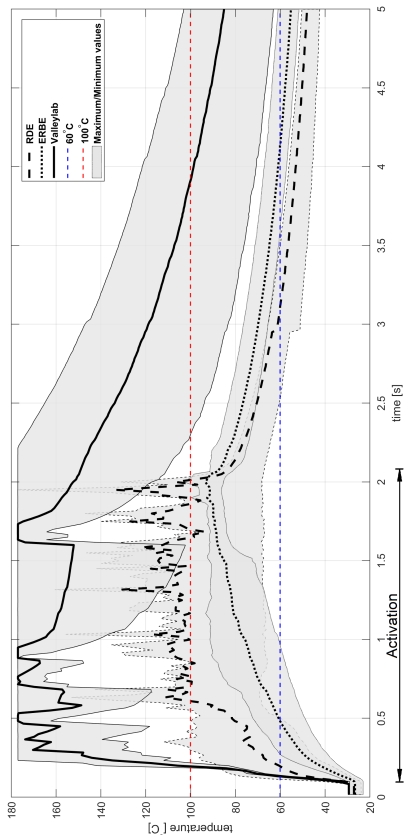
(b) Maximum Temperature over time.

Fig. G.4: Cut; Tofu=3 cm; P=110 W

(a) Area over 50°C and 100°C at every time point.
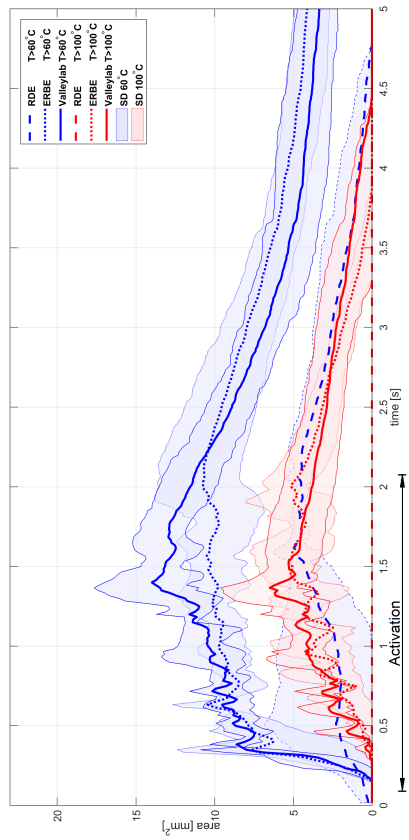
(b) Maximum Temperature over time.

Fig. G.5: Coagulation; Tofu=1 cm; P=40 W

(a) Area over 50°C and 100°C at every time point.

(b) Maximum Temperature over time.

Fig. G.6: Coagulation; Tofu=1 cm; P=70 W

(a) Area over 50°C and 100°C at every time point.
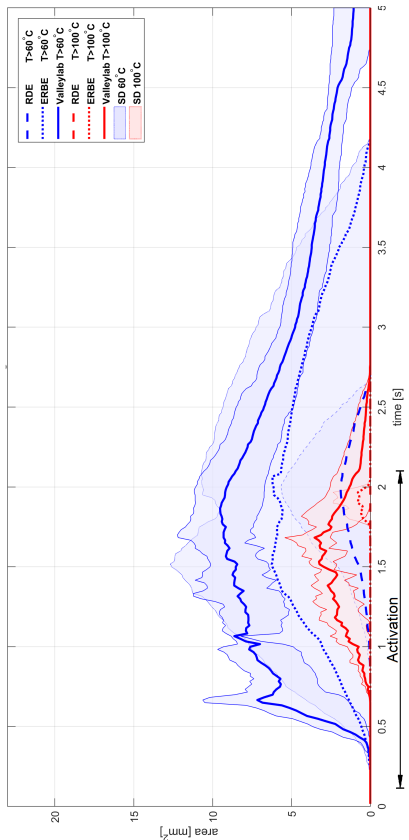
(b) Maximum Temperature over time.

Fig. G.7: Coagulation; Tofu=3 cm; P=40 W

(a) Area over 50°C and 100°C at every time point.

(b) Maximum Temperature over time.
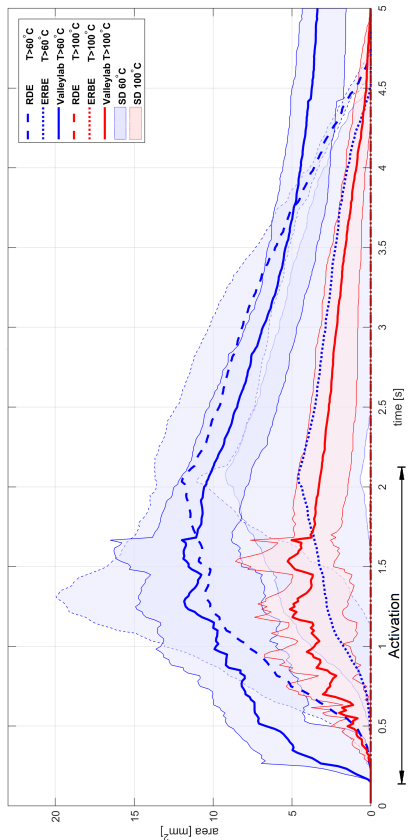
Fig. G.8: Coagulation; Tofu=3 cm; P=70 W

B. Visual TCT Result

Fig. G.9: Photo of all test samples after conducted experiments. Using the Burn Scale in Table IV these samples were analyzed and included in all Thermal Camera Test tables such as Table VII and VIII